

Cite this: *J. Mater. Chem. B*,  
2024, 12, 1706Received 20th August 2023,  
Accepted 4th January 2024

DOI: 10.1039/d3tb01900d

rsc.li/materials-b

## Functional hemostatic hydrogels: design based on procoagulant principles

Boxiang Zhang,<sup>†a</sup> Min Wang,<sup>†a</sup> Heng Tian,<sup>b</sup> Hang Cai,<sup>c</sup> Siyu Wu,<sup>b</sup> Simin Jiao,<sup>d</sup>  
Jie Zhao,<sup>ib</sup> Yan Li,<sup>fg</sup> Huidong Zhou,<sup>b</sup> Wenlai Guo<sup>ib</sup>\*<sup>b</sup> and Wenrui Qu<sup>b</sup>

Uncontrolled hemorrhage results in various complications and is currently the leading cause of death in the general population. Traditional hemostatic methods have drawbacks that may lead to ineffective hemostasis and even the risk of secondary injury. Therefore, there is an urgent need for more effective hemostatic techniques. Polymeric hemostatic materials, particularly hydrogels, are ideal due to their biocompatibility, flexibility, absorption, and versatility. Functional hemostatic hydrogels can enhance hemostasis by creating physical circumstances conducive to hemostasis or by directly interfering with the physiological processes of hemostasis. The procoagulant principles include increasing the concentration of localized hemostatic substances or establishing a physical barrier at the physical level and intervention in blood cells or the coagulation cascade at the physiological level. Moreover, synergistic hemostasis can combine these functions. However, some hydrogels are ineffective in promoting hemostasis or have a limited application scope. These defects have impeded the advancement of hemostatic hydrogels. To provide inspiration and resources for new designs, this review provides an overview of the procoagulant principles of hemostatic hydrogels. We also discuss the challenges in developing effective hemostatic hydrogels and provide viewpoints.

### 1. Introduction

The weight of blood constitutes 7–8% of a healthy adult's body weight and bleeding more than 20% of one's total blood volume at once might result in hemorrhagic shock, organ failure, and even death. Accidental uncontrolled hemorrhage is common in high-risk environments such as battlefields and disasters.<sup>1</sup> Furthermore, heart, liver, spine, and joint surgeries may also result in significant blood loss. Therefore, hemorrhage management in the operating room is critical.<sup>2</sup> Hemorrhage is the leading cause of preventable deaths resulting from trauma.<sup>3</sup> Uncontrolled bleeding caused by trauma accounts for

approximately one-third of pre-hospital deaths, and it remains the second leading cause of death among civilians aged 5–44.<sup>4</sup> Moreover, on the first day of a traumatic accident, approximately 40% of patients die from bleeding.<sup>5,6</sup> Prompt and adequate hemostasis can significantly reduce mortality due to trauma.<sup>7</sup> Conventional methods to stop bleeding include compression, cautery, and surgery, and traditional hemostatic materials, like hemostatic gauze and bandages, have been extensively utilized.<sup>8</sup> However, gauze or bandages must be removed entirely after hemostasis because they do not degrade, which can lead to secondary damage, slower healing, and more discomfort.<sup>9</sup> Recently, polymeric hemostatic materials have provided viable solutions to clinical hemostatic issues. Continuous research has been conducted on enhanced hemostatic materials, including biodegradable hydrogels, sponges, and powders. Hydrogels exhibit good adaptability to irregular wounds.<sup>10</sup> However, some hydrogels are questioned because of their poor biocompatibility or mechanical properties.<sup>11</sup> In addition, hydrogels can realize morphological transformation with sponges, and are endowed with additional shape memory ability.<sup>12</sup> The high water absorption and swelling properties of sponges can endow them with great hemostatic potential,<sup>13</sup> and the most common mechanism by which hemostatic sponges promote coagulation is by absorbing water. In addition, some sponges can also interfere with the physiological mechanism of hemostasis.<sup>14,15</sup> But hemostatic sponges are

<sup>a</sup> Department of Colorectal & Anal Surgery, The Second Hospital of Jilin University, Changchun 130000, Jilin Province, China

<sup>b</sup> Department of Hand Surgery, The Second Hospital of Jilin University, 218 Ziqiang Street, Changchun, 130041, P. R. China. E-mail: guowl19@jlu.edu.cn

<sup>c</sup> Department of Pharmacy, The Second Hospital of Jilin University, Changchun, 130041, P. R. China

<sup>d</sup> Department of Gastrointestinal Nutrition and Hernia Surgery, The Second Hospital of Jilin University, 218 Ziqiang Street, Changchun, 130041, P. R. China

<sup>e</sup> Key Laboratory of Bionic Engineering, Ministry of Education, Jilin University, Changchun, 130022, P. R. China

<sup>f</sup> Trauma and Reparative Medicine, Karolinska University Hospital, Stockholm, Sweden

<sup>g</sup> The Division of Orthopedics and Biotechnology, Department of Clinical Science, Intervention and Technology (CLINTEC), Karolinska Institutet, Stockholm, Sweden

<sup>†</sup> Contributed equally to this work.



easily infected by bacteria.<sup>13</sup> Hemostatic powder can promote hemostasis by absorbing water, sealing wounds, and loading drugs to activate the coagulation cascade. It is worth noting that some hemostatic powders can transform into hydrogels, which improves the portability of hemostatic materials.<sup>16–19</sup> The advantages of powder include convenience, time efficiency, diverse application methods, and suitability for large-area wounds. However, hemostatic powder cannot be applied to noncompressible torso hemostasis.<sup>20</sup>

Ideal hemostatic materials should (1) stop arterial and venous bleeding in large vessels within 2 min; (2) require no prior preparation; (3) be easy to use; (4) be lightweight and durable; (5) be strong enough; (6) be safe; and (7) be inexpensive.<sup>21</sup> Polymeric materials, particularly hydrogels, have shown great potential and garnered interest in hemostasis due to their biocompatibility, flexibility, water absorption, porosity, and multi-functionality.<sup>22–24</sup> However, there are currently only a few hemostatic hydrogels on the market (Table 1) and the extensive data (randomized prospective clinical trials) supporting the efficacy of authorized hemostatic dressings has numerous gaps. Moreover, unclear procoagulant mechanisms may limit the further development of hemostatic hydrogels. For example, patients with coagulopathy cannot be treated with hydrogels that rely solely on the coagulation system to promote hemostasis.<sup>25,26</sup> Thus, this review investigates hydrogel

procoagulant mechanisms. References and design ideas are also offered.

The procoagulant principles of hydrogels will be reviewed in terms of physical and physiological aspects. The former means that through physical features like tissue adhesion,<sup>27</sup> surface charge,<sup>28</sup> and water absorption,<sup>29</sup> hydrogels create an optimal environment for hemostasis. Specific methods include concentrating hemostatic substances<sup>30</sup> and creating physical barriers to seal wounds.<sup>31</sup> The latter means that hydrogel accelerates hemostasis by intervening directly in its physiological processes. Specific methods include intervening blood cells,<sup>28,32</sup> adding coagulation factors<sup>33</sup> and procoagulant substances,<sup>34</sup> and providing additional attachment sites for blood cells.<sup>35</sup> Based on these cells, proteins, and factors mentioned above, functional hydrogels can cater to different hemostatic needs. In addition, numerous studies have been conducted to enhance hemostasis by combining physical and physiological dimensions.<sup>36</sup>

This review sums up the principles of functional hemostatic hydrogels that promote hemostasis along with the features, functional groups, and other components necessary for hydrogels to achieve these principles. Based on the material requirements of the body's coagulation system, we provide inspiration and references for the design of functional hemostatic hydrogels. Furthermore, we discuss the shortcomings or gaps in the current methods of hemostatic function hydrogels for promoting coagulation. Finally, suggestions for possible future directions of functional hemostatic hydrogels are given.



**Boxiang Zhang**

*Boxiang Zhang obtained his Bachelor of Clinical Medicine degree in 2023 from Jilin University, China. Currently, he is a master's student in surgery studying at the Second Hospital of Jilin University, China. His research interests focus on the development of hemostatic materials.*

## 2. Physical hemostasis

Hydrogels promote hemostasis by altering the physical forms of the blood or tissue, referred to as physical hemostasis. The physical forms mainly include localized hemostatic substances' concentration, wound shapes, and the adhesion location of procoagulant substances. Most hemostatic hydrogels have a physical hemostasis function, and these studies highlight properties like high swelling capacity,<sup>37</sup> high tissue adhesion,<sup>38</sup> and vast surface area.<sup>39</sup> Physical hemostasis does not directly intervene in the hemostatic process but rather prepares the way for primary hemostasis.



**Min Wang**

*Min Wang obtained his PhD in surgery from Jilin University, China, in 2011. Currently, he is a professor at Jilin University and a chief physician at the Second Hospital of Jilin University. His research interests focus on the development of hemostatic materials and the diagnosis and treatment of colorectal cancer.*



**Wenlai Guo**

*Wenlai Guo obtained his PhD in surgery from Jilin University, China, in 2019. Currently, he is a lecturer at Jilin University and an attending physician at the Second Hospital of Jilin University. His research interests focus on the development of wound dressings and the repair of extremity nerves.*





Table 1 FDA-approved commercially available hemostatic hydrogels

Materials	Components	Indications	Procoagulant mechanism	Advantages	Limitation
Tegaderm™ alginate dressings	Alginate acid Ca <sup>2+</sup> ion	Cavity wounds Diabetic ulcers Donor sites Leg ulcers Pressure ulcers	Concentration; Ca <sup>2+</sup> ion	Multifunction	Cannot be surgically implanted; Cannot be used on exudating wounds;
HemCon GuardaGel™	Pectin	Minor bleeding from minor topical Cuts and lacerations	Intervention with coagulation cascade	Flexible	Insufficient tissue; Adhesion
Bondilox topical hemostatic dressing	Oxidized cellulose Potassium sorbate Glycerol Ethanol Chitosan fibres Lactic acid	Minor external bleeding Exudate from sutures Controlling moderate to severe bleeding	Physical barrier	—	For trauma use only
BloodSTOP IX Battle Matrix	Regenerated cellulose	External temporary control of minor to moderate bleeding of traumatic wounds.	Physical barrier – adhesion; Intervention with coagulation cascade	Completely soluble in water; Removable	Potential risk of embolism
WoundClot	Modified cellulose	Minor skin surface bleeding wounds such as minor cuts and minor abrasions	Physical barrier – sealing, adhesion	Completely soluble in water; Removable	Non-degradable
Gel-e Flex	Palmitoyl-N-acetyl glucosamine (chitosan)	Local management of bleeding such as lacerations and minor bleeding	Physical barrier	—	The service life is only 28 days
gel-e Flex+ gel OTC	Palmitoyl-N-acetyl glucosamine (chitosan)	Local management of bleeding wounds such as minor cuts, minor lacerations and minor abrasions	Physical barrier	Service life up to two years	Non-degradable

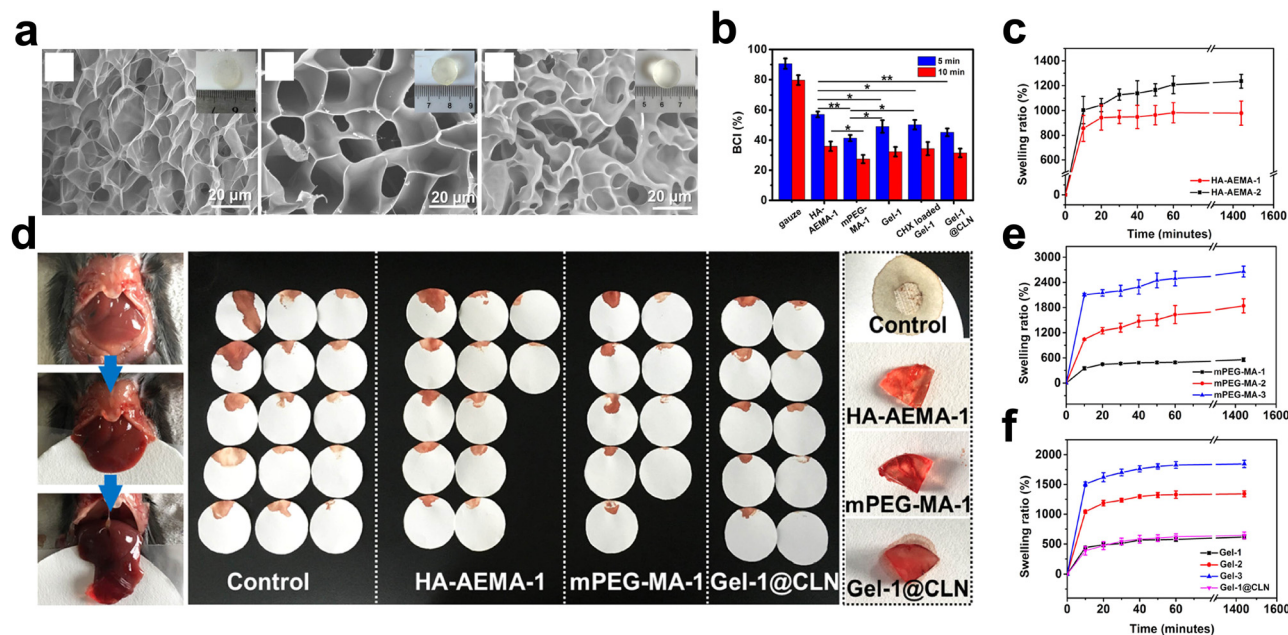


Fig. 1 Application of microporous structured hydrogels based on hyaluronic acid and polyethylene glycol in hemostasis. (a) SEM images of hydrogels. (b) blood-clotting index of hydrogels. (c, e and f) The swelling ratio of hydrogels. (d) Application in the mouse liver injury model. Reprinted from ref. 15 with permission.<sup>29</sup> Copyright 2023 American Chemical Society.

## 2.1. Increasing the concentration of localized hemostatic substances

Increasing the concentration of localized hemostatic substances can promote hemostasis by increasing the contact between various hemostatic substances. By absorbing wound exudate, hydrogels can increase hemostatic substances' concentration. In this review, the two main approaches for designing hydrogels for this function will be discussed: incorporating a porous structure and enhancing hydrophilicity.

**2.1.1. Porous structure.** The porous structure means that the hydrogels have a sponge-like microphysical form through sufficient cross-linking of the materials. Due to their high porosity,<sup>40</sup> hydrogels with porous microstructures have excellent swelling capabilities. Like a sponge,<sup>41</sup> hydrogels concentrate blood through capillary action due to their porous structure. The number of raw materials composed of hydrogels with porous structures is significant, including polysaccharides, proteins, amino acids, and metals.<sup>42–45</sup> Here, we present the hydrogels according to the main cross-linking components that constitute the porous structure.

Hyaluronic acid (HA) is a component of extracellular matrix (ECM) and has high biocompatibility. Zhu *et al.*<sup>29</sup> introduced additional methoxy polyethylene glycol (mPEG) to create a hemostatic synthetic polymer hydrogel to facilitate the control of the structure and material composition of the hydrogel. The results showed that the hydrogel had a porous microstructure and absorbed 1235.27% of its weight of PBS when it reached swelling equilibrium. Moreover, the hydrogel group had lower blood-clotting index (BCI) values than the gauze group, and it controlled hepatic bleeding in mice within 120 s. (Fig. 1) The authors concluded that the porous structure induced by HA and

mPEG led to the excellent absorption capacity of the hydrogel and further promoted hemostasis by concentrating blood.

Chitosan, a polysaccharide derived from marine biological extracts,<sup>46,47</sup> is thought to create porous microstructures by cross-linking. Bal-Ozturk *et al.*<sup>48</sup> generated sponge-like nanostructured hydrogels with interlinked pore structures by cross-linking chitosan, alginate (AA), and the antimicrobial component ZnO. Chitosan is assumed to be primarily responsible for the pore structure. Notably, an acidic environment induces mutual repulsion among the protonated amino groups on chitosan, speeding up the hydrogel's expansion. However, ZnO induces increased intermolecular hydrogen bonding,<sup>49</sup> which compresses the chitosan chains and reduces the material's porosity. Additionally, the increased electron bonding due to ZnO reduces the hydrogel's swelling capacity. Therefore, the authors investigated the optimal content of ZnO for hemostasis. The results of *in vivo* experiments showed that for the rabbit ear peripheral capillary hemorrhage model, the hemostatic time in the experimental group with the minimum amount of ZnO was  $93 \pm 10.41$  s, and the total blood loss was  $263 \pm 168.62$  mg.

Gelatin is an affordable, abundant, and immunogenic alternative to collagen. Additionally, it is frequently utilized to make porous microstructures.<sup>50,51</sup> However, uneven cross-linking can result in fragility for gelatin-based hydrogels created through covalent cross-linking. Physical entanglement enables natural polymers to overcome this flaw. Zainab *et al.*<sup>52</sup> prepared a novel hydrogel gelatin-TA (GelTA) using tannic acid (TA), a plant polyphenol, and gelatin. It is believed that the porous microstructure is one of the causes of the high swelling performance. At a TA concentration of  $0.3 \text{ g ml}^{-1}$ , the porosity of the hydrogel was  $72.1 \pm 6.3\%$ . Excessive TA concentration or an acidic



environment would reduce the porosity and affect water absorption. Moreover, several research studies incorporated nanoparticles with an anisotropic surface charge into the gelatin mixture. For instance, LAPONITE<sup>®</sup> nano clays improve mechanical characteristics by interacting electrostatically with gelatin. The results showed that these hydrogels with a large pore size exhibited good hemostatic efficiency.<sup>53,54</sup>

Silk protein fibre is a cheap, biocompatible, natural protein. Huang *et al.*<sup>55</sup> utilized a cross-linking network of silk fibroin and polyurethane to enhance the porous microstructures. The results showed that the hydrogel's water absorption was increased up to 4.3 times the original value. However, the slow nucleation rate prolonged the preparation time of SF-based hydrogels. Bian *et al.*<sup>56</sup> used biocompatible ethyl lauroyl arginine hydrochloride (LAE) as a surfactant to trigger the gelation of silk proteins. The hydrogel prepared by this method has a hierarchical porous structure, which is believed to contribute to enhanced fluid absorption, and subsequent experimental results showed that this hydrogel absorbed up to 2,898% of its weight of blood in 100 s and possessed good hemostatic capacity.

$\gamma$ -Poly(glutamic acid) ( $\gamma$ -PGA) is a natural homopolymer based on mammalian abundant glutamic acid.<sup>57,58</sup> Chen *et al.*<sup>59</sup> made a hemostatic hydrogel containing  $\gamma$ -PGA-DA, which could absorb water. However, like other *in situ* cross-linked hydrogels, the swelling capacity of  $\gamma$ -PGA-DA was affected by the concentration of the substance or the H<sub>2</sub>O<sub>2</sub> level in the reaction environment. Furthermore, an excessive cross-link density would reduce the swelling capacity by reducing the hydrogel's pore size. Then, SEM images also confirmed this conclusion. *In vivo* experiments demonstrated that the porous structure of  $\gamma$ -PGA-DA accelerated hemostasis.

The swelling potential of cellulose is a result of its thick reticulated structure. Chen *et al.*<sup>60</sup> produced an innovative hemostatic hydrogel by combining cellulose and pectin in an ionic liquid. The liver hemorrhage model's positive hemostatic impact was due to its unique physical structure.

Chondroitin sulfate (CS) is a glycosaminoglycan commonly sulfated in the ECM of human tissues. Zhang *et al.*<sup>61</sup> synthesized a hemostatic hydrogel from CS modified with 5-hydroxytryptamine (5-HT) and serotonin. Serotonin is a procoagulant substance released from activated platelets. The results showed that the hydrogel had an irregular porous structure. The equilibrium swelling of the hydrogel was 68% in 12 h when the polymer concentration was 2 wt%. The hydrogel stopped bleeding the mouse liver hemorrhage model in about 30 s.

Arista is an absorbable hemostatic particle with a microporous structure originating from inert plants, which has a wide range of applications in the field of surgery.<sup>62</sup> Inspired by Arista, Cui *et al.*<sup>63</sup> developed a new hydrogel with a swelling rate higher than 2000% based on carboxy starch carboxylic starch. In another study, the hydrogels formed by grafting acrylic acid (AAc) and acrylamide (AAm) onto starch achieved swelling rates of up to 18000%, as reported in the results.<sup>64</sup>

Metal-organic gels (MOGs) are novel metal-organic materials with porous microstructures. Inspired by MOGs, Yang *et al.*<sup>45</sup>

created a multifunctional hydrogel with hemostatic properties by combining Zn<sup>2+</sup> and 4,5-imidazole dicarboxylic acid. The SEM pictures revealed that this hydrogel has linked porous microstructures, which were believed to be responsible for swelling. Unfortunately, the results of the swelling test were not included in this study.

The hydrogel's porous microstructure aids in fluid absorption to promote hemostasis. However, for hydrogels formed by covalent bonding, excessive cross-linking or uneven microstructure distribution will reduce the porosity of the hydrogel, which will further reduce the hemostatic substances' concentration ability.<sup>48</sup> Second, the multifunctional hydrogels' porosity may be influenced by various materials. Thus, the appropriate ratio of raw materials is also worth considering. Finally, it is crucial to evaluate whether a significant increase in hemostatic substances' concentration can lead to either wound dryness or excessive blood loss.

**2.1.2. High hydrophilicity.** Hydrophilic surfaces have a strong affinity for water molecules.<sup>65</sup> Increased hydrophilicity aids the hydrogel in concentrating blood, hence accelerating hemostasis. Hydrophilic groups like amino,<sup>66</sup> carboxyl,<sup>67</sup> and hydroxyl,<sup>68</sup> or hydrophilic substances such as mesoporous silica,<sup>69</sup> mineral kaolin, aluminum silicate,<sup>70</sup> and zeolite, can be incorporated into hydrogel systems to enhance hydrophilicity.

Carboxyl is a common hydrophilic group.  $\gamma$ -PGA has carboxyl groups in its side chain, allowing it to be grafted with various functional groups.<sup>67,71</sup> Moreover,  $\gamma$ -PGA is suitable for manufacturing hemostatic materials due to its hydrophilicity. In a study on  $\gamma$ -PGA and poly(lysine),<sup>66</sup> the positively charged amino in the system imparted good hydrophilicity to the hydrogel, and this new hydrogel achieved excellent concentration properties for hemostatic substances.

A superabsorbent polymer was synthesized by grafting a hydrophilic carboxymethyl group and acrylic acid onto chitosan.<sup>43,72,73</sup> The water absorption capacity of the modified hydrogel was improved, and the swelling ratio of this hydrogel in distilled water could exceed 900. Besides, a novel hydrogel was synthesized from carboxymethyl chitosan and kappa-carrageenan, a highly hydrophilic sulfated polysaccharide polymer derived from seaweed,<sup>74,75</sup> which is believed to promote hemostasis by concentrating blood. However, swelling test results for this hydrogel were not reported.<sup>76</sup>

A commonly used component for enhancing hydrophilicity is the hydroxyl group. Some hydrogels have been treated using hydroxyl-rich compounds to increase their water absorption. Luo *et al.*<sup>77</sup> synthesized a gelatin-based hemostatic hydrogel. The hydrogel was modified using dopamine (DA), *N*-hydroxy succinimide (NHS), and HA. HA is hygroscopic,<sup>78</sup> DA possesses a polyphenolic structure, and NHS is hydrophilic. The results showed that the water contact angle of the hydrogels decreased from the initial  $102.5 \pm 3.5^\circ$  to  $61.2 \pm 2.6^\circ$ , (Fig. 2) which proved that the hydrogel achieved better hydrophilicity. Polar groups like hydroxyl, carboxyl, and amino<sup>79</sup> are thought to increase the hydrogels' hydrophilicity.

Besides introducing hydrophilic functional groups, substances with excellent hydrophilicity have been extensively used



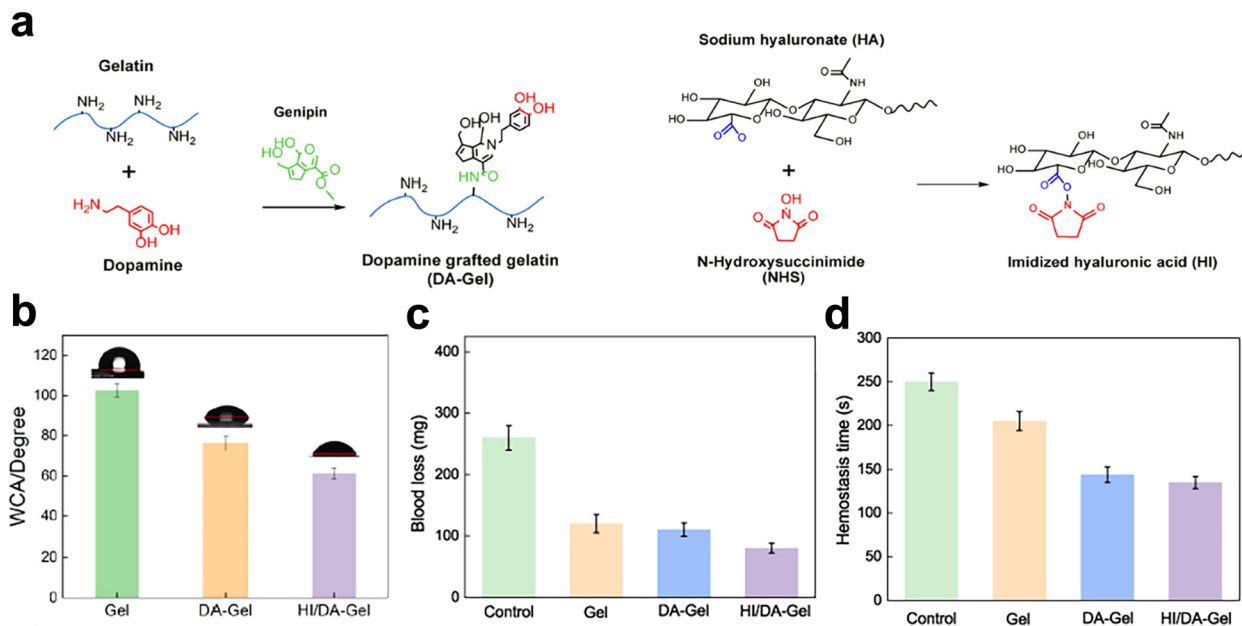


Fig. 2 Gelatin enhanced hydrophilic and hemostatic effects by grafting hydrophilic substances. (a) and (b) Dopamine, *N*-hydroxy succinimide, and HA were grafted onto gelatin. (c) The water contact angle of hydrogels. (d) and (e) Blood loss and hemostasis time of hydrogels. Reprinted from ref. 63 with permission.<sup>77</sup> Copyright 2022 Elsevier.

to improve the water absorption of hemostatic hydrogels. Bovine serum albumin (BSA), a biocompatible natural protein, has great hemostatic potential due to its hydrophilicity, but its weak mechanical qualities restrict its applicability. Wang *et al.*<sup>80</sup> added the inorganic salt NaCl to BSA to facilitate the gelation process by shielding the electrostatic repulsion between BSA molecules, resulting in the better water-holding capacity of the hydrogel. This BSA-based hydrogel's equilibrium swelling water content reached 76%. Hydroxyethyl cellulose (HEC), a non-ionic natural cellulose ether, exhibits good hydrophilic characteristics due to the presence of abundant hydroxyl groups.<sup>68</sup> Wang *et al.*<sup>81</sup> introduced mesoporous silica (with a porous structure and high specific surface area) based on quaternized HEC<sup>69</sup> to synthesize the quaternized HEC/mesoporous silica foam (MCF) hydrogel sponge (QHM). The highest swelling ratio of this material reached  $7013.4 \pm 310.4\%$ .

In a study examining hemostatic hydrogels focusing on water absorption and mechanical properties,<sup>82</sup> the double bond of polybutadiene is grafted with poly(acrylic acid) (PAA) through free-radical polymerization to increase the water absorption capacity of the hydrogel. The results indicate that glassy polystyrene imparts strength to the hydrogel, while polybutadiene imparts rubbery ductility. This nanophase-separated structure enables the hydrogel to swell an order of magnitude faster than other hydrogels. Poly(ethylene glycol) (PEG) is a non-toxic, non-immunogenic material widely used in tissue engineering scaffolds.<sup>83</sup> Moreover, PEG is considered an excellent hemostatic material due to its porous structure and hydrophilic nature, which can absorb large amounts of water from serum.

Furthermore, the design of a 4-arm PEG hydrogel, based on PEG, is a new research direction in recent years.<sup>84</sup> The 4-arm PEG-based hydrogel achieved a swelling rate of up to 1790%.

*In vivo*, experiments showed that bleeding from a 3 cm diameter and 1 cm depth porcine skin laceration model could be stopped within 30 s. One of the reasons for hemostasis was thought to be the high swelling rate.<sup>85</sup> Poly(vinyl alcohol) (PVA) hydrogels have good hydrophilicity, biocompatibility, and degradability<sup>86</sup> and have been used to manufacture hemostatic hydrogels due to their hydrophilicity.<sup>87</sup>

The major components of kaolinite are mineral kaolinite and aluminum silicate,<sup>70</sup> and the well-known trauma dressing QuikClot Combat Gauze (QCCG) contains kaolinite. Inspired by QCCG, Tamer *et al.*<sup>88</sup> cross-linked PVA with kaolin, and the physical structure of the hydrogel was thought to improve the poor absorption of QCCG for osmosis. The results showed that this hydrogel absorbed  $365 \pm 15\%$  water after 1 h. Zeolite, an aluminosilicate mineral with tunable hydrophilicity,<sup>89</sup> can rapidly concentrate blood from the site of injury. Besides, some studies posit that because zeolite has coagulation factor V and coagulation factor X on its surface, which are considered precursors for the synthesis of thrombin, zeolite can accelerate hemostasis by accelerating the physiological mechanism of hemostasis.<sup>90</sup> However, the exothermic reaction of zeolite in use limits its application.<sup>91</sup> Recently, the heat-release phenomenon that occurs when zeolite promotes hemostasis has been solved.<sup>92</sup> Fathi *et al.*<sup>93</sup> combined zeolite with chitosan and alginate. The objective was to exploit chitosan's biocompatibility to compensate for zeolite's drawbacks. At 1 h, the group without zeolite absorbed more PBS solution than those with zeolite. However, adding zeolite significantly increased the material's absorption capacity at 5 or 10 min, which was considered more practical. Furthermore, the zeolite group could clot whole sheep blood within 15 s, while the alginate group took 5.5 min, and the chitosan-loaded alginate group took about 2 min.



Hydrogels are modified to enhance their hydrophilicity, facilitating their ability to increase hemostatic substances' concentration and thus promoting hemostasis. However, some studies suggest that the removal of hydrophilic hemostatic dressings after achieving hemostasis may pose difficulties, such as a risk of secondary injury like more bleeding.<sup>94,95</sup> Besides, it remains to be studied whether excessive striving for hydrophilicity can lead to excessive blood loss.

## 2.2. Establishing a physical barrier

Hydrogel promotes hemostasis by adhering or sealing bleeding wounds, which is called the physical barrier of hemostasis. Traditional emergency hemostatic modalities like electrocautery can harm tissue.<sup>96</sup> Moreover, traditional hemostatic methods have limited effectiveness on irregular or deep wounds.<sup>97</sup> It may be more beneficial to use hydrogels to overcome these difficulties. Hydrogel adhesion to a bleeding wound is the most common way to achieve it.<sup>98,99</sup> Many materials improve adhesion.<sup>32,100–102</sup> Tissue sealing requires the hydrogel to have the ability to adapt to different shapes. This review will describe these hydrogels according to tissue adhesion and tissue sealing. More information on physical barriers can be found in Table 2.

**2.2.1. Tissue adhesion.** Adhesion results from the interaction between tissue and hydrogels, and various studies have improved the tissue adhesion of hydrogels by grafting functional groups based on polysaccharide substrates or protein substrates.<sup>31,103</sup> Hemostatic hydrogels with adhesive functions can not only be applied to surface wounds but can also be used *in vivo*, such as endoscopic nasal hemostasis or ulcerative arterial bleeding. Not only this, some studies have pointed out that hemostatic hydrogels also have broad application prospects on the mucosal surface of the digestive tract.<sup>104–106</sup> Hydrogels adhere to wounds to stop bleeding. These hydrogels are better for emergency hemostasis in ruptured arteries or other fast bleeding.<sup>107</sup> Typically, adhesive hydrogels have high mechanical strength and adhere to various material surfaces (Fig. 3). This review presents existing studies based on the functional groups that enhance the adhesion of tissues.

Hydrogels can achieve adhesion function by using the phenolic moiety, which has a strong binding affinity for nucleophiles in human tissues<sup>108</sup> and can form covalent connections with amino and sulfhydryl groups in tissues. The phenolic moiety is dispersed on polydopamine,<sup>109</sup> TA,<sup>110</sup> gallic acid (GA).<sup>111</sup> The number of phenolic groups on the molecular backbone of TA is high.<sup>112</sup> Increasing the TA proportion in the hydrogel system can significantly improve tissue adhesion.<sup>113</sup> For example, a TA-based hydrogel showed a maximum adhesion strength of 68.2 kPa to porcine skin and a good hemostasis effect in a liver hemostasis model with a blood loss of only 0.07 g.<sup>114</sup> To overcome the challenge of creating hydrogels from pure polyphenolic chemicals, Shao *et al.*<sup>115</sup> produced a hemostatic hydrogel using thioctic acid as a macromolecular spacer and TA of phytic acid. Results from shear-tension experiments show that this hydrogel can adhere to various material surfaces. However, the oxidation of phenolic hydroxyl groups leads to

reduced adhesion. Therefore, it is necessary to control the phenolic hydroxyl group oxidation.<sup>99</sup>

Hydrogel adhesion is improved by catechol, a benzene derivative with two adjacent phenolic groups. Metal ions bind with catechol, improving mechanical characteristics. Wang *et al.*<sup>116</sup> added Fe<sup>3+</sup> to catechol-functionalized chitosan (CCS) to induce catechol-Fe<sup>3+</sup> chelation. This double cross-linking mechanism increased the possibility of linking the material with amino, thiol, and imidazole covalent groups. The lap shear strength between the hydrogel and the porcine skin was 18.1 kPa. Polyphenols can also create dynamic covalent connections with boron (B<sup>3+</sup>) and ferric ions (Fe<sup>3+</sup>).<sup>117</sup> Self-polymerizing dopamine yields polydopamine (PDA).<sup>118</sup> Phenyl boric acid engages in an electrostatic interaction with the amino group on chitosan. A boronic ester bond links the catechol and boronic acid groups.<sup>119</sup> These two reasons together improve the mechanical properties of the hydrogel.<sup>42</sup> Based on these parameters, a chitosan-based hydrogel was created, exhibiting an adhesion strength of 27.6 kPa to porcine skin<sup>120</sup> and demonstrating excellent hemostasis in a liver hemorrhage model. Zhong *et al.*<sup>121</sup> used catechol to modify the four-arm PEG with many sulfhydryl groups, significantly improving wet tissue adhesion and mechanical strength by inducing the Michael addition reaction. Furthermore, in a study of CCS with PEG,<sup>122</sup> the hydrogels could withstand burst pressures over 120 mmHg. Catechol and aldehyde groups are believed to work together to provide excellent tissue adhesion.

Besides catechol, substances containing catechol structures can also enhance adhesion. The bioactive substance 3,4-dihydroxy-L-phenylalanine (DOPA) with catechol found in mussel secretions is a good choice for improving adhesion.<sup>123</sup> Xie *et al.*<sup>124</sup> grafted DOPA onto gelatin methacryloyl, which significantly improved the adhesion of the hydrogel to the surface of various wet tissues (*e.g.*, porcine skin, heart, and lungs). The *in vivo* experiments showed that the hydrogel facilitated rapid wound closure. Moreover, Yan *et al.*<sup>125</sup> modified poly(L-glutamic acid) with DOPA to improve the mechanical properties of hydrogels. The results showed that the adhesion strength was 28.3 ± 3.1 kPa. Hydrogel can be a physical barrier to stop bleeding due to its increased catechol content, improving wet tissue adhesion. To address the limitation of poor tissue adhesion of pure HA hydrogels, grafting DOPA is a common approach,<sup>126,127</sup> and the modified hydrogels have a good barrier effect on arterial, venous, and irregular wound bleeding.

Adhesive hydrogels can quickly create Schiff base bonds with tissue amino groups.<sup>128</sup> Dodecyl aldehyde is a substance commonly used to enhance adhesion. Moreover, after modification with this substance, the hydrophobic aliphatic side chains of the hydrogel can insert into the cell membranes of porcine skin,<sup>129</sup> a process known as hydrophobic interactions. Hydrophobic and aldehyde groups promoted adhesion,<sup>130</sup> for example, in a study with a chitosan-based hydrogel. The results showed a maximum adhesion strength of 20.43 ± 0.71 kPa.<sup>131</sup> Besides chitosan, aldehyde groups are also used to enhance the adhesion of HA-based hydrogels.<sup>132</sup> Furthermore, in a study of oxidized carboxy-methyl cellulose (OCMC) and ECM, OCMC



Table 2 Hydrogels with physical hemostasis function

Hydrogels	Material composition	Chemical modification/addition	Characterize	Characterize realization mechanism	Animal model	Ref.
Increasing localized hemostatic substances' concentration	Multifunctional CODM hydrogel	Polyvinylpyrrolidone Dopamine Chitosan	Oxidized alginate-modified Carboxymethyl-modified -NH <sub>2</sub>	Swelling ratio: 481.2 ± 8.6% Protamine increases crosslinking density	Rat femoral artery bleeding model	237
	PEG-CMC-THB-PRTM hydrogel	Montmorillonite Chitosan	Carboxymethyl-modified aldehyde group 2,3,4-Trihydroxy	Swelling ratio > 10 times	Rat liver hemorrhage model	238
	CAO/ATR hydrogel	Polyethylene glycol Phenyl aldehyde Protamine Chitosan	Carboxyethyl-modified Silver	High porosity and swelling ratio (2078% ± 244%)	-OH groups on TA increased affinity for water adsorption Physical interactions between polymer chains and silver-tannic acid nanoparticles (Ag-TA NPs)	239
	PCbM wound dressing	Sodium alginate (OSA) Tannic acid Polyvinyl alcohol Chitosan	Ag ion Cu ion	Swelling rate is about 60% Water contact angle: 18° ± 3° Swelling ratio: 41.09 ± 2.68 g g <sup>-1</sup>	AgCu metal-organic frameworks reduces the crosslinking density	Rat liver and tail hemorrhage model
COP hydrogel	Chitosan Dextran	Carboxymethyl-modified Oxidized	Swelling ratio: 230.8%	γ-Glutamic acid has high absorbency	Rat tail hemorrhage model	241
HG-CB@R hydrogel	Poly-γ-glutamic acid Hyaluronic acid	β-Cyclodextrin-grafted Bisphosphonate groups	Swelling ratio: 282 ± 4.1 mmHg	Iron-affinitive BP groups enhance swelling performance	Rat liver bleeding, heart puncture, tail vein bleeding model and femoral artery bleeding model	242
Physical barrier	G-P15/HA-P1/G-Q1/HA-NB0.4	Hyaluronic acid	PNIPAM-grafted gelatin (G-P) Maximum burst pressure of 282 ± 4.1 mmHg	Abundant polar functional groups(-OH, -NH <sub>2</sub> , and -COOH) form intensive hydrogen bonds with the polar groups on the tissue surface. The -CHO forms a dynamic Schiff base with the primary -NH <sub>2</sub> on gelatin and the tissue surface The β-sheet structures of gelatin is helpful to exposure of -OH, -NH <sub>2</sub> ,	Mouse liver puncture model	243
Tissue	Gelatin	The quaternary ammonium modified gelatin (G-Q)				
Adhesion	CMCS/ODex/γ-PGA (COP) hydrogel	The PNIPAM-grafted HA (HA-P) The o-nitrobenzyl (NB) modified HA (HA-NB). Carboxymethyl-modified Oxidized	The complete gelation time is 18.49 ± 2.77 s	Triple-network structure: The intramolecular amide bonds The intermolecular amide bonds The Schiff base bonds The structure of PDA is similar to mussel-adhesive proteins and adheres to many organic and inorganic surfaces	Rat liver hemorrhage model	244
	FCMCS/rGO/PDA multi-component system	Chitosan Polydopamine (PDA) Graphene oxide (GO) Maleic hyaluronic acid	Carboxymethyl-modified Adhesive strength is about 34 kPa			245
DMHA hydrogel		Catechol-modified	Maximum adhesive force of ~55 N	Hydrogen bonds formed between catechol dihydroxy and amines or hydroxyl groups UV photopolymerization between acrylate and thiol groups	Rat liver injury model Rabbit femoral artery bleeding model	246





Table 2 (continued)

Hydrogels	Material composition	Chemical modification/addition	Characterize	Characterize realization mechanism	Animal model	Ref.
CMCS/PD hydrogel	Chitosan Polyaldehyde dextran	Carboxymethyl-modified	Burst pressure: 327.5 ± 9.3 mmHg	A large number of aldehyde groups on the hydrogel are anchored to amino groups on the tissue	Rat liver hemorrhage model rat tail severance model rabbit liver and cardiac hemorrhage models	247
levan-catechol hydrogel	Levan	Catechol-modified	Adhesive strength: 42.17 ± 0.24 kPa	Covalent and non-covalent bonds between nucleophiles group on tissue, and hydroxyl with catechol groups, oxidized o-quinone groups, hydroxyl groups	rat liver perforation wound models	248
Tetra-PEG-NHS hydrogel	Gelatin PEG	Amino-modified Tetra-armed	Ruptured pressure: 55 kPa	Succinimidyl-active ester moieties tightly bound to amino groups on the tissue surface	Rabbit arterial, hepatic, and carotid diaphragm models	249
H(C-A/OD)/TA/HNT2 hydrogel	Chitosan Dextran tannic acid	carboxymethyl-modified Oxidized Halloysite nanotubes				
Physical barrier Tissue sealing	GelMA-SW-ZF nano-composite sealants	Methacryloyl-modified	Injectable	Shape adaptability	Rat liver and artery bleeding models	250
	Zinc ferrite		Shorter gelation time	ZF and SN mediate the generation of hydrogen bonds and electrostatic interactions		
CGD hydrogel	Silicate nanoplatelets Chitosan	Dihydrocaffeic acid (DHCA) β-glycerophosphate	Burst pressure is about 30 kPa Injectable	Arboxylate and hydroxyl groups of DHCA and β-glycerophosphate enhance chitosan thermogelation	Rat hepatic hemorrhage and tail amputation models	251
GelDA/DAGNC/Ca <sup>2+</sup> /Fe <sup>3+</sup> hydrogel	Gelatin Cellulose	Catechol-conjugated Dialdehyde-modified Ca <sup>2+</sup>	Injectable Self-adaptability	Double dynamic bonds in the hydrogel network	Rat tail amputation, liver bleeding Rabbit ear artery, liver bleeding models	252
CQCS@gel	Chitosan	Fe <sup>3+</sup> Catechol-functionalized quaternized	Injectable	Catechol groups bond with moieties (e.g., amines, thiols) in tissue surfaces <i>via</i> Schiff base reaction and Michael addition	Rat-tail amputation, liver hemorrhage and carotid bleeding models	253
T-STH hemostats	Poly(ethylene glycol)	Dibenzaldehyde-terminated	Self-healing	Dynamical reversible Schiff-base linkages could re-form at the broken sites		
Tri-BA@PVA/G	Poly(N-isopropyl acrylamide) Poly(vinyl alcohol) Boric acid	Silicate nanoplatelets	Adhesive strength: 33.5 ± 7.8 kPa Burst pressure: 146 mm Hg Injectable	Shear-thinning properties	Rat liver bleeding model	254
		Guanosine K <sup>+</sup> ion	Injectable Shape adaptation ability	A large number of dynamic chemical bonds inside the hydrogel network	Rat liver hemorrhage model	255

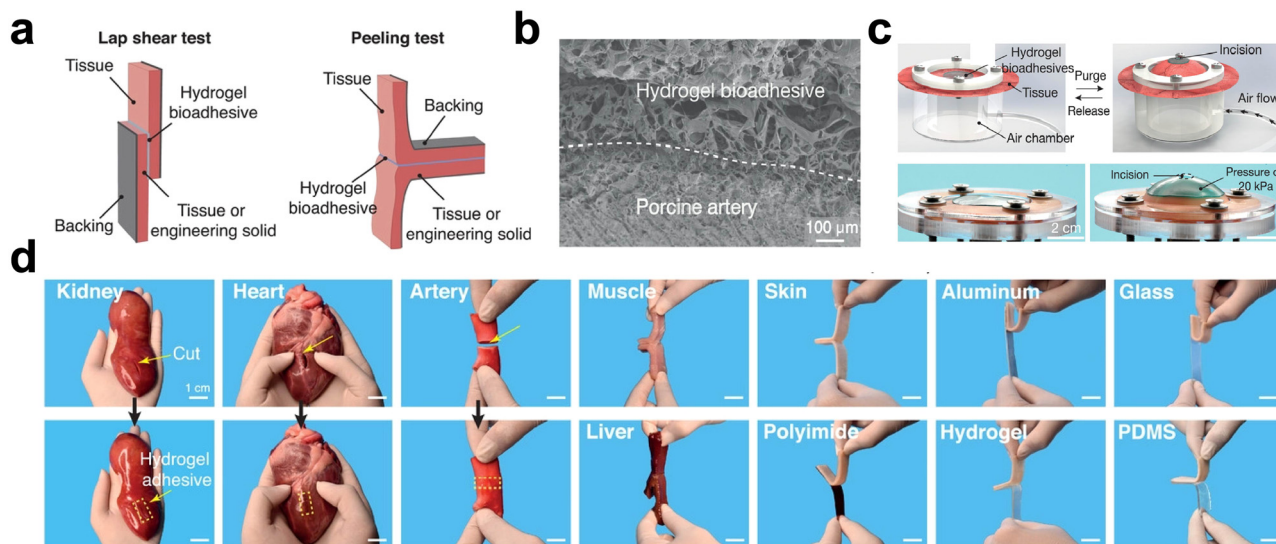


Fig. 3 Adhesion performance of the hydrogel. (a) Schematic of hydrogel adhesion verified by lap shear and 180° peeling tests. (b) SEM images of hydrogel-adhered porcine arterial tissue (scale bar: 100 μm). (c) Photograph of a hydrogel undergoing a bursting pressure test (scale bar: 2 cm). (d) Photographs of hydrogels adhering to a variety of surfaces. Reprinted from ref. 88 with permission.<sup>107</sup> Copyright 2021 Wiley.

could form imine bonds with the intrinsic amines of ECM, and the number of aldehyde groups in the hydrogel backbone was considered critical for adhesion properties.<sup>133</sup> This OCMC-based hydrogel exhibited a maximum adhesion strength of  $185 \pm 10$  kPa and a burst pressure of  $14.58 \pm 0.32$  kPa.

Hydroxyl groups can interact chemically with amino groups or amide bonds in tissues and enhance the adhesion of hydrogels.<sup>99</sup> The hydroxyl groups in starch, cellulose, and HA are abundant. Two phenolic acids that are abundant in nature are protocatechuic acid (PA) and glyoxylic acid (GA), with GA having one more hydroxyl group than PA in its structure.<sup>134</sup> In one study, GA and PA were grafted onto gelatin to form two hydrogels: GEG (GA-engineered gelatin) and PEG (PA-engineered gelatin).<sup>135</sup> The adhesion strengths of the two hydrogels were 35.1 and 28.3 kPa, respectively. Specifically, the additional hydroxyl groups promoted the formation of more Schiff bases between gelatin and histone proteins, which could be the reason for improved adhesion.

Urea groups can promote hydrogen bond formation and thus enhance the hydrogels' tissue adhesion. Zhang *et al.*<sup>136</sup> synthesized IEM-Gln using L-glutamine and 2-isocyanate ethyl methacrylate (IEM). Ordered hydrogen bonds are formed in the presence of urea groups. Acrylamide (AM) and IEM-Gln undergo polymerization through various hydrogen bonds, resulting in the formation of a new polymer hydrogel. The results show that this hydrogel adheres to numerous material surfaces, with an average adhesion strength of 6.7 kPa to pig skin. Multiple hydrogen bonds and electrostatic interactions contribute to good adhesion. This hydrogel also promoted hemostasis in a rat liver damage model with 91 mg blood loss by acting as a physical barrier (Fig. 4).

Hydrogels can enhance tissue adhesion by grafting a variety of functional groups. However, these functional groups must remain stable to prevent any performance failures. Moreover,

there is a need to explore whether super adhesion makes the removal of hydrogels difficult. Finally, hydrogels that achieve a physical barrier function by adhering to tissue should have enhanced mechanical properties.

**2.2.2. Tissue sealing.** Conventional hemostatic hydrogels face difficulty in completely covering irregular wounds, resulting in inadequate hemostasis.<sup>137</sup> Tissue sealing intends to fill or plug bleeding wounds with hydrogels to promote hemostasis. In recent years, tissue-sealing hydrogels have been rapidly developed to address the hemostasis needs of irregularly shaped and deep wounds.<sup>138</sup> Some swellable hydrogels can fill wounds and impede blood flow by expanding.<sup>139</sup> Besides, some hydrogels usually take the form of *in situ* synthesis or injection to adapt to the shape of the wound.<sup>140</sup> This review will present the existing studies based on the application of hydrogels in tissue sealing.

Swellable hydrogels can fill the wound to block blood flow. One study added flaxseed gum to a cellulose system to synthesize a cellulose/flaxseed gum composite hydrogel with over 200% moisture expansion.<sup>139</sup> Another study synthesized pectin/cellulose hydrogels. *In vivo*, experiments demonstrated the outstanding hemostatic properties of the two hydrogels discussed above. It was believed that the creation of a physical barrier contributed to the promotion of hemostasis. Furthermore, starch has several applications in hemostasis. Zeinab *et al.*<sup>141</sup> synthesized a hydrogel with high swelling properties by grafting AAC and AAm on starch. The *in vivo* experiments showed that this hydrogel swells rapidly and blocks blood flow in the rat femoral artery by forming aggregates.

*In situ* formed hydrogels have the inherent advantage of acting as a physical barrier. However, they exhibit limitations in terms of mechanical strength and suitability for emergency use. Yu *et al.*<sup>142</sup> intended to improve these defects by applying more hydrogen bonds. The hydrogel stopped bleeding within 8 s in a liver bleeding model, reducing bleeding by 92.56%. Additionally,



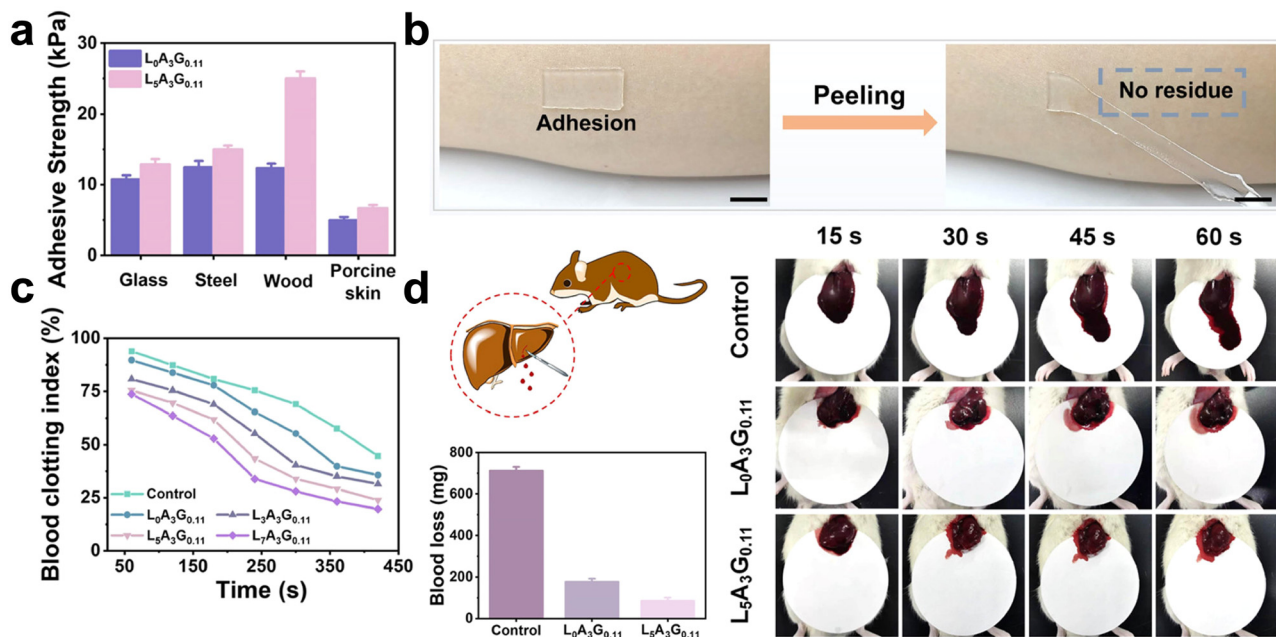


Fig. 4 A hemostatic hydrogel that exerts an adhesion effect. (a) The adhesion strength of hydrogels to different materials. (b) Photograph of hydrogel, scale: 10 mm. (c) Dynamic whole-blood-clotting evaluation of hydrogels. (d) *In vivo* hemostatic properties of hydrogels, including schematic diagrams of rat liver injury models, photographs of liver blood loss, and comparisons of blood loss. Reprinted from ref. 117 with permission.<sup>156</sup> Copyright 2021 American Chemical Society.

aldehyde hydroxyethyl starch (AHES) and amino carboxymethyl chitosan (ACC) combined to form an *in situ* AHES/ACC hydrogel with hemostatic function through a Schiff base reaction. The *in vivo* hemostatic experiment exhibited that the AHES/ACC

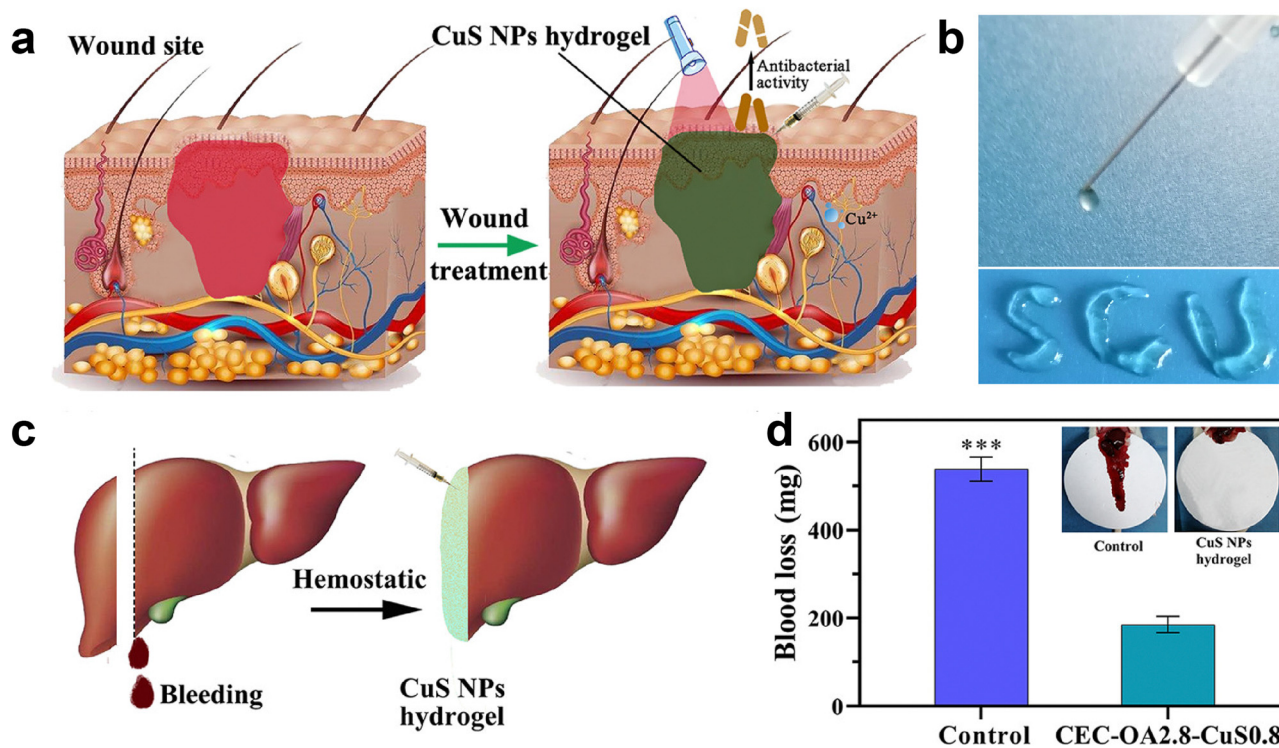


Fig. 5 Hydrogel promotes hemostasis by sealing wounds. (a) Schematic diagram of hydrogel sealing a bleeding wound. (b) Photograph of the injectable hydrogel. (c) and (d) Schematic diagram of the injectable hydrogel applied to hemostasis in a liver injury model and comparison of blood loss. Reprinted from ref. 126 with permission.<sup>145</sup> Copyright 2021 American Chemical Society.



hydrogel formed a physical barrier on the wound through its three-dimensional network structure. This *in situ* hemostatic mechanism controls bleeding and blood loss effectively.<sup>143</sup> Luo *et al.*<sup>140</sup> also created an *in situ* formed HA/gelatin hydrogel. Burst pressure testing results determined the hermeticity of the hydrogel, and the burst pressure was measured to be  $24.71 \pm 11.58$  kPa. Moreover, the blood loss in the rat liver hemorrhage model using the HA/G hydrogel was  $120.4 \pm 149.5$  mg, approximately 50% less than the negative control group.

Injectable hydrogels are more adaptable to irregular wounds, and the four-armed PEG has better mechanical strength than linear PEG.<sup>144</sup> Huang *et al.*<sup>121</sup> produced a hydrogel utilizing benzaldehyde-terminated four-arm poly(ethylene glycol) grafted with carboxymethyl chitosan. This hydrogel was believed to be synthesized and sealed at the wound site. In the hemostasis test, the hydrogels flowed into the wound and could seal it with a hemostasis time of  $120 \pm 10$  s and a blood loss of  $0.29 \pm 0.11$  g. The wound's movement may lead to the tearing of the hemostatic dressing. A hemostatic injectable hydrogel was synthesized using *N*-carboxyethyl chitosan and oxidized sodium alginate. This hydrogel can self-heal due to the formation of Schiff base bonds by the abundant amino and aldehyde groups. In the rat hepatic hemorrhage model, the hydrogel was significantly successful at stopping bleeding, and the bleeding volume was approximately one-third that of the control group (Fig. 5). The physical barrier effect was responsible for the exceptional hemostatic effect.<sup>145</sup>

Hydrogels can block blood flow by sealing a wound, which requires the hydrogel to be swellable or flowable. Notably, *in situ*-formed hydrogels are more difficult to manipulate during the application,<sup>146</sup> which may not meet the requirements for emergency hemostasis. Furthermore, it is yet to be investigated whether hydrogels that fill the tissue by swelling can cause wound damage or discomfort. Finally, a hemostatic hydrogel with self-healing qualities helps reduce dressing tears caused by transportation or activity, making it more appropriate for use in emergencies.

### 3. Physiological hemostasis

The hemostatic process was roughly divided into three stages: vasoconstriction, primary, and secondary hemostasis.<sup>147</sup> When a blood vessel ruptures, mediators such as endothelin and platelet-derived thromboxane A<sub>2</sub> (TXA<sub>2</sub>)<sup>148,149</sup> and the neurogenic reflex mechanisms of the blood vessels themselves, induce myogenic contraction of the blood vessel wall, resulting in a reduction in the local blood flow rate and bleeding volume. The primary hemostasis occurs in the first 3 to 7 min after vessel rupture,<sup>150</sup> producing platelet thrombi.<sup>151</sup> Tissue factors (TF) released from the damaged vessel may also initiate secondary hemostasis; thus, secondary and primary hemostasis may start simultaneously.<sup>152,153</sup> Principal components of secondary hemostasis include the successive activation of coagulation factors, production of thrombin, and conversion of fibrinogen to fibrin.<sup>154</sup> A fibrin clot reinforces the platelet thrombus formed

during primary hemostasis.<sup>153</sup> Thrombin is an allosteric serine protease with coagulation activity. It is an essential component of the hemostasis system.<sup>155</sup> Fibrin develops from insoluble fibrin monomers. The latter is produced when thrombin converts soluble fibrinogen into fibrin.<sup>156</sup>

The physiological process of hemostasis involves interactions between various extracellular ligands, soluble proteins, platelet receptors, coagulation factors, and fibrin.<sup>157–159</sup> Hydrogels that can activate the hemostatic system directly have been designed based on these substances. Reducing the elapsed time for the aggregation of coagulation substances is the core problem that hemostatic materials must solve. The complex mechanism of the coagulation physiological process and numerous hemostatic substances provide numerous targets for hydrogels to promote hemostasis. Therefore, there are many types of hydrogel materials with this function.<sup>160–162</sup> This review classifies the available hydrogel hemostatic interventions into the following categories: the intervention of platelets, RBCs, and the initiation of the intrinsic pathway.

#### 3.1. Intervention with platelets

Primary hemostasis relies on platelets. After vascular rupture, exposed subcutaneous collagen adheres to and activates some platelets *via* the large transmembrane protein integrin on the platelet surface.<sup>163,164</sup> Moreover, the damaged vascular endothelium exposes a soluble plasma glycoprotein, von Willibrand factor,<sup>165,166</sup> which can lead to a small amount of platelet adhesion.<sup>167</sup> The plasma membrane in the region near the binding site responds to the shear forces of blood flow, leading to the activation of these platelets.<sup>159,168,169</sup> Activated platelets extend many pseudopodia and release the contents of internal granules, mainly 5-HT, intrinsic adenosine diphosphate (ADP), and TXA<sub>2</sub>.<sup>170–172</sup> The above vasoactive chemicals activate other platelets, which repeat the same process to increase platelet aggregation. Finally, platelets generate a thrombus at the vascular injury site to complete primary hemostasis.

Direct intervention in the physiological state of platelets can promote hemostasis more quickly and directly. It is a method by which hydrogel intervenes in primary hemostasis. Hydrogels are designed to attract and activate platelets through surface charge, increased platelet adhesion sites, and the provision of bioactive substances. This review classifies platelet-interfering hydrogels based on electrostatic interactions, attachment site provision, and the addition of bioactive substances.

**3.1.1. Electrostatic interactions.** Platelets possess a negative surface charge. The positive surface charge can attract and activate platelets in the hydrogel. This method is efficient and practical.

Amino groups are commonly positively charged groups. There is an electrostatic interaction between the negative charge on the surface of the blood cells and the positive surface charge of the hemostatic material. Liu *et al.*<sup>173</sup> introduced aminated silver nanoparticles to a gelatin system, and the hydrogel's hemostatic properties were enhanced by the protonated amino group. The amino group on the backbone of chitosan is among the fundamental reasons for its inherent hemostatic ability.<sup>174</sup>



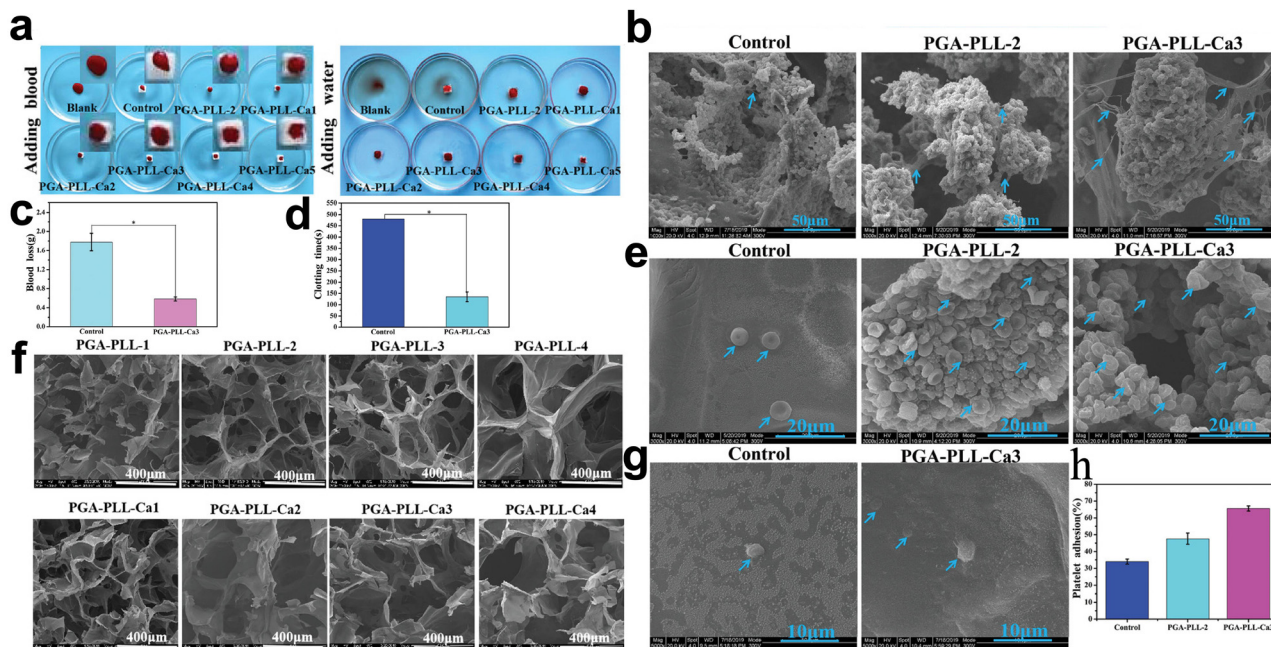


Fig. 6 Application of poly(glutamic acid), poly(lysine), and calcium ion-based multifunctional PGA-PLL-Ca composite hydrogels in hemostasis. (a) Photograph of the hydrogel after adding 100 μl of whole blood dropwise and adding 20 ml of deionized water dropwise and incubating for 5 minutes. (b) SEM images of hydrogels after absorption of whole blood. (c) and (d) Blood loss and clotting time in rat liver injury models. (e) and (g) SEM images of erythrocytes and platelets attached to the hydrogel surface. (f) SEM images of lyophilized PGA-PLL hydrogels with different cross-linker concentrations. (h) Platelet adhesion quantification. Reprinted from ref. 52 with permission.<sup>66</sup> Copyright 2021 Wiley.

Zheng *et al.*<sup>175</sup> proposed a hydrogel containing quaternary ammonium chitosan that reduced blood loss by 80% in a liver injury model. SEM images showed aggregated platelets on the hydrogel's surface. In another study on chitosan, *in vitro* experiments measured a minimum BCI of  $82.19 \pm 1.19\%$ . This hydrogel was thought to have better hemostatic properties. However, the results of *in vivo* experiments were not reported.<sup>176</sup>

Synthetic silica nanoplatelets exhibit a favorable charge distribution with positive charge at the surface edges and negative charge at the top and bottom.<sup>177</sup> Combining gelatin with this nanomaterial, Gaharwar *et al.*<sup>178</sup> produced a hydrogel. Platelet aggregation was observed on the surface of the hybrid hydrogel, which was not observed on gelatin alone. Electrostatic or hydrophobic interactions have been proposed to explain this phenomenon.<sup>179</sup> *In vivo*, hemostasis tests showed that this hydrogel significantly reduced bleeding. Moreover, LAPONITE<sup>®</sup> (LP), a common nano silicate, has been widely used to boost physiological hemostasis. For example, in a study of polyglutamic acid, a moderate amount of LP could reduce blood loss from 872 to 88 mg in a rat liver hemorrhage model, significantly improving the hemostatic performance.<sup>180</sup>

The positively charged surface of certain antimicrobial peptides (AMPs) confers antibacterial action. Additionally, they increase platelet adhesion. Atefyekta *et al.*<sup>181</sup> synthesized a hydrogel using AMPs and performed an *in vitro* coagulation test using whole human blood. Results showed that AMPs induced significant platelet agglutination.

Substances with a positive surface charge are frequently employed to stimulate the physiological changes in platelets. This is a frequent and efficient method.

**3.1.2. Provision of attachment sites.** During hemostasis, platelets act by sticking to the wound site. Hydrogels can increase hemostasis by providing additional attachment sites for platelets at the wound site, thus facilitating the production of hemostatic plugs. Various studies aim to realize this function through network structure, membrane receptors, or interaction.<sup>182</sup> This review describes these studies regarding hydrogels providing sites for platelet adhesion.

Hydrogels with high porosity can facilitate platelet adhesion. The scanning electron microscopy images (SEMs) of these hydrogels show porous microstructures and numerous platelet adhesion sites (Fig. 6). Since most hydrogels inherently possess a networked structure, numerous materials can provide platelet adhesion sites. For instance, gelatin-based hydrogels have been developed to increase surface porosity and homogeneity with smaller hole sizes, resulting in superior platelet adhesion.<sup>44</sup> Moreover, chitosan is utilized more frequently due to its inherent porosity.<sup>183,184</sup> The morphological characterization of these hydrogels is confirmed by SEM images. Zhang *et al.*<sup>183</sup> synthesized a hydrogel using sericin, chitosan, and PVA as the backbone, and TEM images showed a perforated structure on the surface of the hydrogel. The *in vitro* coagulation experiments showed that the blood co-incubated with this hydrogel had the lowest absorbance, indicating the best coagulation properties of the material. Numerous aggregated activated platelets were visible on the hydrogel surface in SEM images. Furthermore, molecular cross-linking agents, like cysteamine-modified chitosan, can improve the three-dimensional structure of the hydrogel.<sup>185</sup>



Receptors on the platelet cell membrane or membrane surface can also anchor platelets. In a study involving a cell adhesive peptide conjugate (Pept-1),<sup>182</sup> hemostasis was accelerated through the binding of platelet surface  $\alpha$ 8bb3 receptors to RGD moieties on Pept-1. Chen *et al.*<sup>186</sup> also attached blood cells by complexing carboxyl groups with  $\text{Fe}^{3+}$  in the blood cells. *In vitro*, coagulation assays revealed low BCI values, and scanning electron micrographs revealed that this hydrogel had a strong ability to adsorb blood cells.

Hydrogels are also capable of attaching and reacting with platelets. For instance, undecanal-modified chitosan, a hydrophobically modified chitosan, has hydrophobic fatty side chains that bind to the hydrophobic interior of platelets, generating a robust hemagglutination reaction.<sup>174</sup> Chen *et al.*<sup>187</sup> also prepared hemostatic hydrogels using similar logic, and dodecyl-modified chitosan contributed to an excellent anchoring effect on platelets.

Hydrogels can offer a greater surface area, receptors, and interactions to support platelet attachment compared to wounds. Further research is needed to determine whether thrombus loosening and further bleeding occur upon the removal of platelet-loaded hemostatic hydrogels.

**3.1.3. Addition of bioactive substances.** Nearly all physiological hemostasis processes include platelet physiological changes, and the high density of membrane surface receptors makes it possible for several bioactive compounds to target platelets.<sup>159,167,171</sup> Hemostatic hydrogels that directly incorporate bioactive substances capable of acting on platelets have emerged recently.

Keratin, a natural structural protein, possesses intrinsic hemostatic properties, and keratin is believed to mediate platelet adhesion through integrins and has found wide application in the field of functional hemostatic hydrogels.<sup>188,189</sup> In a study involving keratin-based hydrogels, the *in vitro* hemostatic time of the hydrogels was reduced to 12 min compared to 15 min in the control group. The *in vivo* experimental results showed a 56.8 and 60.7% reduction in blood loss in the experimental group at 30 and 120 s, respectively. The authors attribute this to keratin's inherent characteristics.<sup>190</sup> Moreover, Burnett *et al.*<sup>35</sup> synthesized a hemostatic keratin hydrogel. Notably, the active portion of integrins was partially blocked by antibodies, which significantly decreased the platelet adsorption capacity of the hydrogels, providing further evidence of integrin-mediated platelet adhesion. However, keratin can be used not only as a substrate but also as an additive product to promote hemostasis. Sun *et al.*<sup>191</sup> incorporated keratin into fibrin-based hydrogels. The hemostasis effect of the hydrogel was twice that of fibrin.

ECM, composed of collagen, glycoproteins, and glycosaminoglycan, is a biologically active substance capable of directly activating platelets.<sup>192</sup> Ventura *et al.*<sup>193</sup> prepared ECM hydrogels by a lyophilization method. The highest ECM group had the lowest BCI and maximum platelet adhesion. The authors determined that this substance may be the finest gelatin substrate. Human-like collagen (HLC), derived from collagen, is a material with excellent biocompatibility and low

immunogenicity.<sup>194</sup> In one study, chemically modified HLC was added to an HA-based hydrogel. The results of the hemostasis test showed that the hydrogel effectively stopped acute hemorrhage in the liver, reducing the amount of bleeding from approximately 750 to 15 mg.<sup>195</sup>

Platelet-dense granules contain natural platelet-activating ADP. Liu *et al.*<sup>174</sup> created a hydrogel using ADP, HA, and chitosan. ADP-modified HA activated platelets through P2Y12 receptors. In particular, the experimental group with added ADP showed the best coagulation effect on platelet-rich plasma (PRP).

There are numerous activation mechanisms for platelets, and most bioactive chemicals that promote physiological changes in platelets are endogenous. Platelet particles contain numerous platelet-activating substances that can be used in hemostatic hydrogels.

### 3.2. Intervention with RBCs

As the most abundant blood cells, RBCs do not play a significant role in the traditional physiology of hemostasis. However, there is growing body of evidence that RBCs play a role in hemostasis and thrombosis.<sup>196</sup> Hematocrit and blood flow conditions are physical manifestations of the procoagulant effect of RBCs, and a low hematocrit may result in reduced significant thrombosis.<sup>197</sup> Moreover, RBCs are associated with many cells or molecules that perform hemostatic functions. For example, RBCs adhere on the endothelium of the vessel wall under certain conditions,<sup>198</sup> direct cellular contact of RBCs with platelets and promotion of thrombosis,<sup>199</sup> a fibrin-related aggregation of RBCs,<sup>200,201</sup> and the regulation of formed clots and thrombi *in vivo* by RBCs.<sup>202</sup> More detailed mechanisms have been revealed in the following reviews.<sup>203,204</sup>

Hydrogels interfere with red blood cells in three ways: electrostatic interactions,<sup>43</sup> including bioactive chemicals, and supplying attachment sites.<sup>205</sup> We have listed some studies that can interfere with red blood cells in a table (Table 3).

### 3.3. Intervention with the coagulation cascade

The coagulation cascade reaction is the main element of secondary hemostasis in the coagulation mechanism, and this reaction is a critical event in the massive production of thrombin (Fig. 7). Hydrogels can interfere with the physiological processes of the coagulation cascade by affecting the levels of coagulation factors or other substances in the wound environment. The number of hemostatic hydrogels able to intervene in the coagulation cascade has expanded steadily in recent years. These investigations have heavily relied on the precise chemicals loaded for their intended purpose. This review describes these hydrogels according to three perspectives: initiation of the intrinsic pathway,<sup>206</sup> addition of coagulation factors, and addition of bioactive substances.

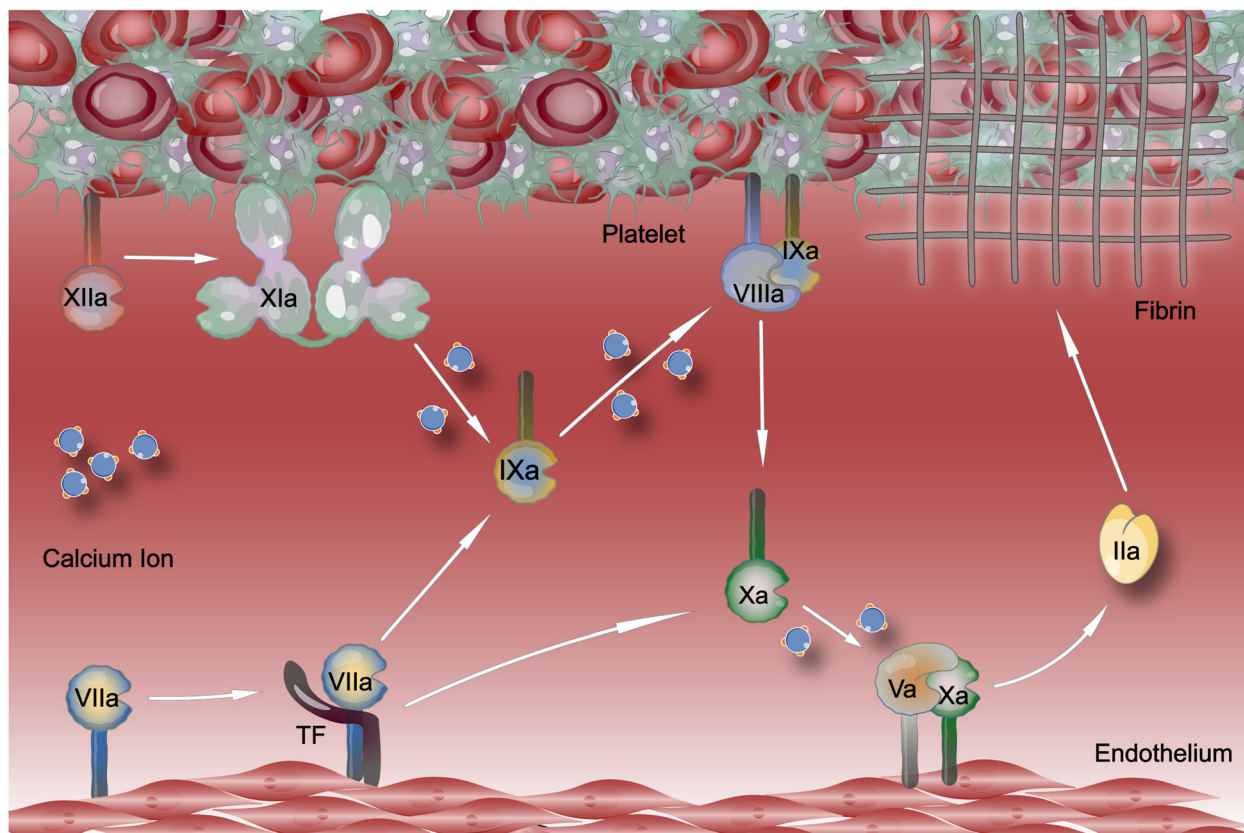
**3.3.1. Initiation with the intrinsic pathway.** The coagulation cascade is an autocatalytic reaction between coagulation factors. The specific process automatically activates more post-cascade factors by activating pre-cascade factors. The coagulation cascade is currently separated into intrinsic and extrinsic



Table 3 Hydrogels that promote hemostasis by interfering with red blood cells

Materials	Mechanisms	Functional substance	Verification Methods	Ref.
Silk fibroin/chitosan	Electrostatic interaction	The amino groups of chitosan	BCI	256
Catechol-modified oxidized hyaluronic acid/aminated gelatin/Fe <sup>3+</sup>	Electrostatic interaction	The amino group in aminated gelatin	—	257
<i>N</i> -Citraconyl-chitosan/acrylates/arginine	Electrostatic interaction	Chitosan/arginine	—	258
Chitosan/gelatin/polyvinyl alcohol	Electrostatic interaction	Chitosan	BCI	259
Gelatin/dextran/ethylenediamine	Electrostatic interaction	Ethylenediamine	BCI/SEM	260
3-Carboxy-phenylboronic acid/gelatin/poly(vinyl alcohol)	Electrostatic interaction	3-Carboxy-phenylboronic acid	BCI/SEM	261
Sodium alginate/hemoglobin/carbon quantum dots	Addition of bioactive substances	Sodium Iginate/hemoglobin	BCI/SEM	34
Hydroxybutyl chitosan/chitosan/dopamine	Addition of bioactive substances	Dopamine	SEM	262
Dopamine/modified poly(l-glutamate)	Addition of bioactive substances	Dopamine	Red blood cell attachment/BCI	263
Porcine acellular dermal matrix	Addition of bioactive substances	Extracellular matrix	BCI	264
Gelatin methacrylate/adenine acrylate/CuCl <sub>2</sub>	Addition of bioactive substances	Gelatin	—	265
Carboxymethyl cellulose/dopamine	Provision of attachment sites	Dopamine	BCI/SEM	186
Four-armed benzaldehyde-terminated polyethylene glycol/dodecyl-modified chitosan/vascular endothelial growth factor	Provision of attachment sites	Dodecyl-modified chitosan	—	187
Short peptide RG-5/halloysite nano-tubes/Alginate/gelatin	Provision of attachment sites	Halloysite nano-tubes	—	266
Poly(vinyl formal)	Provision of attachment sites	Poly(vinyl formal)	—	267
Catechol derivatives/gelatin derivatives/ureido-pyrimidinone	Provision of attachment sites	Ureido-pyrimidinone	BCI	268

(BCI: blood-clotting index; SEM: scanning electron microscope)



**Fig. 7** The coagulation cascade. The intrinsic pathway begins with FXIIa (F refers to factor, a refers to activated), and then FIX is activated, and FVIIIa activates FX along with FIXa, and the latter two reactions require the involvement of calcium ions. The extrinsic pathway begins with the formation of a complex between FVII and tissue factor (TF); then FIX and FX are activated by the complex, and FIXa binds to FVIIIa and activates FX, leading to the convergence of the intrinsic and extrinsic pathways. FXa can form a prothrombinase complex with FVa in the presence of calcium ions, and eventually fibrin is formed.



pathways.<sup>207</sup> Blood is the source of all coagulation factors in the intrinsic pathway.<sup>208</sup> It is typically triggered by contact between negatively charged surfaces or collagen and blood.<sup>209</sup> Coagulation factor FXII (a serine protease produced in the liver)<sup>210</sup> is activated to FXIIa (F refers to factor, a refers to activated) upon binding to the surface of a foreign body, which then triggers a subsequent cascade reaction. The extrinsic pathway is initiated by external TF.<sup>211</sup> These two reactions converge when thrombin is formed.<sup>212</sup> Thrombin then catalyzes the generation of fibrin from fibrinogen, increasing the platelet thrombus's stability. Physiological mechanisms of the intrinsic pathway have inspired several recent studies on hemostasis.

Substances of biological origin can activate intrinsic pathways *via* FXII. Silk proteins were thought to be capable of initiating the endogenous coagulation pathway by activating FXII.<sup>213</sup> Bai *et al.*<sup>108</sup> combined TA with silk protein, and this hydrogel can stop the bleeding in a rat liver hemorrhage model with a blood loss of only  $35.2 \pm 8.6$  mg. HLC is also similar to collagen, an artificial substance synthesized from human collagen cDNA fragments.<sup>214</sup> Shang *et al.*<sup>215</sup> synthesized a hemostatic hydrogel using HLC and investigated the HLC effect on the initiation of the coagulation cascade. The kit measured the amount of FXII, and the results showed that the FXII secretion was significantly increased in the liver wounds of the hemorrhage model in the experimental group. This hydrogel design strategy is thought to promote hemostasis by increasing FXII.

Some studies have also initiated intrinsic pathways through some negatively charged substances. Kappa carrageenan was used as a coating for the starch/cellulose nanofiber system, and the results of *in vitro* coagulation experiments showed that this strategy achieved lower BCI values. The authors concluded that the negative charge on the hydrogel surface promoted the FXII activation, further enhancing the hydrogel's coagulation function. Nonetheless, a more conclusive investigation of the source of the negative charge on the hydrogel surface must be conducted.<sup>216</sup> Besides, synthetic silicate nanoplatelets have also been used to initiate coagulation cascades due to their negatively charged surfaces.<sup>136,217</sup> Gaharwar *et al.*<sup>178</sup> used gelatin as a substrate to piggyback synthetic silicate nanoplatelets. The results of *in vitro* coagulation experiments showed that the clotting time of this hydrogel was reduced by up to 77% compared to the control group. Furthermore, mesocellular silica was also used in the study due to its similar properties.<sup>81,206</sup> Notably, the FXII-mediated coagulation cascade is not triggered at low MCF concentrations. Besides, kaolin (the main component is aluminum silicate) can also initiate the coagulation reaction by activating FXII and has been used to make hemostatic hydrogels.<sup>218,219</sup>

Hydrogels can promote hemostasis by activating the intrinsic pathway of the coagulation cascade through FXII. However, some studies only intervene in the coagulation cascade and do not activate platelets. The coagulation cascade is a series of protein hydrolysis reactions on the activated platelets' surface.<sup>220</sup> It must be determined whether hydrogels that merely intervene in the coagulation cascade will result in insufficiently activated platelets, diminishing their ability to promote hemostasis.

**3.3.2. Addition of the coagulation factor.** The coagulation factor is a general term for more than ten species of substances directly involved in coagulation. The coagulation cascade aims to produce thrombin and promote fibrin formation. Facilitating the accelerated synthesis of thrombin at a faster rate has been a difficulty for hemostasis materials. By skipping some earlier steps in the coagulation cascade, the direct injection of coagulation factors may allow the reaction to proceed more quickly. Hydrogels can promote hemostasis by releasing coagulation factors, accelerating the coagulation cascade.  $\text{Ca}^{2+}$  (FIV) is an essential component of the prothrombinase complex<sup>220</sup> and is vital in the coagulation cascade and plays a significant role in the coagulation cascade. Adding  $\text{Ca}^{2+}$  to hydrogel systems is relatively easy. Currently, the most common coagulation factor used in functional hemostatic hydrogels is  $\text{Ca}^{2+}$ .<sup>221</sup>

In research on hemostatic hydrogels with added  $\text{CaCl}_2$ , the absorbance of the hydrogels in the experimental group increased and then declined with increasing  $\text{Ca}^{2+}$  concentration, indicating that the hydrogels' hemostatic capacity increased and then reduced.<sup>66</sup> The authors concluded that the reason for this phenomenon is that the formation of blood clots increases with increasing  $\text{Ca}^{2+}$  concentration, which hinders the  $\text{Ca}^{2+}$  release within the system. Therefore, hydrogels with this hemostatic function must be used with attention to uniform  $\text{Ca}^{2+}$  release. Cheng *et al.*<sup>222</sup> added nanoscale  $\text{Ca}(\text{OH})_2$  to carboxymethyl chitosan, a sodium alginate-based system formed through ion cross-linking, aiming to solve the contradiction between the stable preservation and rapid release of  $\text{Ca}^{2+}$ . The results show that  $\text{Ca}(\text{OH})_2$  formed under alkaline conditions can stably store more  $\text{Ca}^{2+}$ . The authors concluded that the acidic blood flowing from the wound further promoted the rapid release of  $\text{Ca}^{2+}$  from  $\text{Ca}(\text{OH})_2$ .

Current methods of hydrogel intervention in the coagulation cascade must be significantly improved. The coagulation cascade is a complicated reaction involving dozens of components<sup>223</sup> and offers various hydrogel intervention sites. However, current studies are limited to initiating the reaction or adding a single coagulation factor, which may be limited by technical conditions. It should be noted that more than just relying on  $\text{Ca}^{2+}$  alone may be required to accelerate the coagulation cascade. The addition of more clotting factors may be a more efficient approach.

**3.3.3. Addition of bioactive substances.** Some hydrogels are designed to accelerate hemostasis by adding bioactive substances that promote the coagulation cascade. Most bioactive substances are associated with cells that secrete coagulation substances during the coagulation process, such as poly(phosphate) (PolyP), DNA, or some amino acid chains. Among them, PolyP has recently attracted increasing attention.

PolyP is a macromolecule composed of repeating phosphate units.<sup>224,225</sup> Human platelets contain this bioactive substance, and PolyP is associated with FXI activation. The polymerization degree also influences the physiological effects of PolyP.<sup>226–228</sup> PolyP can be added by coupling to a hydrogel backbone without a substrate. Chen *et al.*<sup>229</sup> combined polyP with poly(aspartic hydrazide) (PAH) to form a novel hydrogel that reduced blood



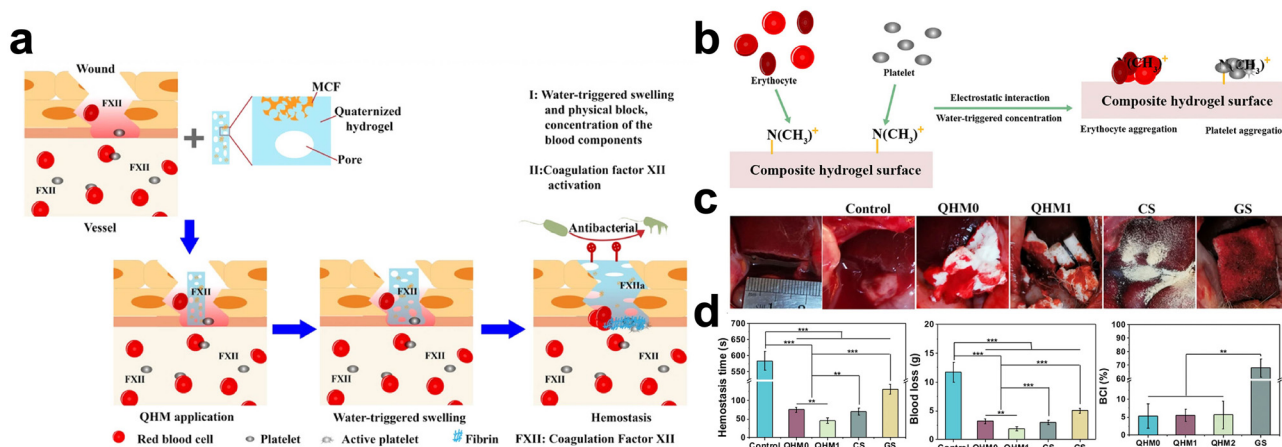


**Fig. 8** Quaternized hydroxyethyl cellulose and mesocellular silica foam-based hydrogels for hemostasis. (a) Schematic diagram of a hydrogel that promotes hemostasis by concentrating blood, attracting red blood cells and platelets and activating coagulation factor FXII. (b) Schematic diagram of hydrogel attracting red blood cells and platelets. (c) Hemostatic behavior of hydrogels in a rabbit liver injury model. (d) Hemostasis time and blood loss in rabbit liver injury models, blood clotting indexes (BCI) of various hydrogels *in vitro* experiments. Reprinted from ref. 67 with permission.<sup>81</sup> Copyright 2019 American Chemical Society.

loss in rabbit ear arteries by 71.2% and hemostasis time by 68.6%. A hydrogel loaded with PolyP was synthesized,<sup>230</sup> and the results of *in vivo* testing showed a 69.96% reduction in hemostasis and a 74.79% reduction in hemostasis time in the treated group. Moreover, in a study on HA-based hemostatic hydrogels,<sup>231</sup> the PolyP introduction increased the clotting rate, an indicator of clot mechanical strength, by 1.5-fold. The authors concluded that PolyP accelerates fibrin clot formation. The fibrin clot is among the end products of the coagulation cascade and is indirect evidence of the physiological effects of PolyP. Cao *et al.*<sup>232</sup> synthesized a PolyP/TA hydrogel, and the BCI values of all the hydrogels in the experimental group containing PolyP were less than 20%. Blood loss in the experimental group's mouse hepatic hemorrhage model was just 10% of the blank groups. The above results demonstrated the procoagulant properties of PolyP.

DNA is also used in hydrogels to promote hemostasis. For example, TA was used as a substrate, and DNA was added to synthesize a hemostatic hydrogel.<sup>112</sup> The *in vivo* hemostasis test showed that this hydrogel could stop bleeding in the mouse liver in approximately 53 s, while the blank group required about 133 s. However, a fully DNA-based hydrogel lacked procoagulant action, indicating that the idea that DNA promotes hemostasis requires further exploration.<sup>233</sup>

In recent years, several new materials have evolved, including short peptides. Some short peptides have hemostatic action. For example, the ideal amphipathic peptide (IAP), a combination of leucine and lysine residues, has been used to prepare functional hemostatic hydrogels. Charbonneau *et al.*<sup>234</sup> synthesized a novel hydrogel using IAP and quantified FIX, FX, and thrombin using ELISA kits. Specifically, IAP promoted the activity of these essential molecules in the coagulation cascade. The *in vivo* results showed that this hydrogel was effective in hemostasis in various hemorrhage models. A modified chitosan backbone was used to carry I3QGK, an ultrashort peptide

with hemostatic activity, to form a hydrogel.<sup>184</sup> Interestingly, the hydrogel could cause a rapid loss of fresh whole blood fluidity when the concentration of I3QGK was maintained above at least 5.03 mg ml<sup>-1</sup>, demonstrating the extreme procoagulant ability of the hydrogel.

As a cascade reaction, the coagulation cascade comprises multiple components and is simple to initiate. The addition of bioactive chemicals makes hydrogels a prospective option for interfering with the coagulation cascade.

## 4. Synergistic hemostasis

The effect of promoting hemostasis by a single procoagulant mechanism may be limited. In recent years, some high-level studies have promoted hemostasis in physical and physiological ways, which is a better solution.<sup>81,103,235,236</sup>

Hydrogels can have several procoagulant characteristics and induce hemostasis through a synergistic action. Typically, these hemostatic hydrogels exhibit significant swelling or tissue adherence. Besides, they can also interfere with blood cells and coagulation cascades. (Fig. 8) For example, in a hemostatic study, a hydrogel with synergistic hemostatic function can increase hemostatic substances' concentration, adsorb, and activate platelets, attract RBCs, and activate coagulation factor FXII, which all contribute to the excellent hemostatic effect. In addition, we have listed some studies (Table 4). It is worth mentioning that promoting hemostasis by exerting synergistic effects may be the future development direction of hemostatic hydrogels.

## 5. Conclusion and outlooks

Stopping uncontrollable bleeding is challenging in high-risk environments like battlefields, disasters, and operating rooms.





Table 4 Hydrogels that promote hemostasis through synergistic action

Materials	Procoagulant mechanisms	Animal models	Hemostasis time and blood loss	Ref.
Chitosan	Physical barrier; provide attachment sites; intervention with RBCs; intervention with coagulation cascade	The mouse liver hemorrhage model	< 50 s (liver)	269
Alginate	Concentration; physical barrier; intervention with blood cells; intervention with coagulation cascade	The rabbit-ear artery model; the rabbit-liver bleeding model; the rat-tail amputation model; the rat-liver injury model	97 ± 14 s, 215 ± 19 mg (ear); 81 ± 16 s (liver); 222 ± 11 s (tail)	222
Bletila striata polysaccharide	Concentration of blood; physical barrier	The mouse-tail amputation model; the mice-liver injury model	81.0 ± 8.8 s, 59.92 ± 10.9 mg (tail); 60.8 ± 4.2 mg (liver)	270
Cellulose	Concentration of blood; intervention with blood cells; intervention with coagulation cascade	The rat-tail amputation model; the rabbit-liver lethal defect model	45 ± 8 s (liver)	81
Gelatin	Concentration of blood; intervention with blood cells; intervention with coagulation cascade	The mice-tail amputation model; the mice-tail amputation model	19.6 mg, 56 s (liver); 26.8 mg, 65 s (tail)	232
Polyacrylamide	Concentration of blood; physical barrier; Intervention with platelets	The rat liver puncture model The rat tail amputation model; the ovine liver laceration model	Reduced by 1 minute on average (rat liver); reduced by 12 minutes on average (ovine liver)	271
Polyethylene glycol	Physical barrier; intervention with blood cells	The rat-tail amputation model	The blood loss decreased 10.3 times, the hemostasis time decreased 4.2 times	272
Chitosan	Intervention with palates; physical barrier	The mouse liver trauma model; the mouse liver incision model; the mouse-tail amputation model	143.9 ± 60.3 mg (liver trauma); 207 ± 19.3 mg (liver incision); 30 ± 4.0 mg (tail amputation)	38
Poly(ethylene glycol)	Physical barrier; intervention with RBCs	The mouse hemorrhaging liver model; the mouse heart bleeding model	0.037 mg (liver); greatly decreased blood loss compared to the blank group (1.08 g)	273
Poly(ethylene glycol)	Physical barrier; concentration of blood	The mouse liver bleeding model	41.1 ± 15.2 mg	274

Traditional means of hemostasis are difficult to meet the need for hemostasis due to several drawbacks. Therefore, there is a need to develop materials that promote hemostasis. Recently, polymeric materials, particularly hydrogels, have shown great potential for hemostasis. However, commercially available hemostatic hydrogels are insufficient in stopping bleeding quickly and have a limited range of application. Therefore, these materials cannot satisfy emergency situations' hemostatic needs and unique groups' needs. Numerous functional hemostatic hydrogels capable of promoting hemostasis through several procoagulant processes have been produced by researchers. This review describes several procoagulant mechanisms of hydrogels: First, hydrogels can change the physical forms of the blood or tissue near the wound to create conditions for hemostasis. The physical forms include hemostatic substances' concentration, wound shapes, and the adhesion location of procoagulant substances. To achieve these functions, hydrogels with a porous structure, hydrophilicity, swelling, mobility, or tissue adhesion are required. Second, hydrogels can directly promote hemostasis by intervening in the physiological mechanisms of hemostasis. RBCs, platelets, and the coagulation cascade are crucial for the physiological processes of hemostasis. Achieving these functions requires hydrogels with surface charge, large surface area, or the ability to load multiple bioactive substances. Finally, hydrogels can exert physical and physiological procoagulant functions through synergistic effects. In conclusion, the existing hydrogels are comprehensive in their procoagulant mechanisms and exhibit excellent hemostatic ability.

However, there are still areas for improvement in the design and development of hemostatic hydrogels. First, the high increase in hemostatic substances' concentration may result in wound drying or excessive blood loss, rendering the hydrogel inappropriate for use in young children with low blood volume. It is crucial to select a more effective physiological procoagulant mechanism to develop a hydrogel. Second, some hydrogels are difficult to remove, leading to secondary injury or bleeding. Therefore, selecting more appropriate interactions between tissue and hydrogel is necessary when enhancing tissue adhesion. Third, some hydrogels compress the wound causing discomfort, so it is necessary to improve the shape adaptability of the hydrogel. Fourth, hydrogels that solely intervene in the physiological process of hemostasis may face challenges in stopping bleeding in coagulation-problem patients successfully. Therefore, synergistic hemostasis may represent the future of hemostatic hydrogel development.

In conclusion, elucidating the procoagulant mechanism may provide ideas for improving functional hemostatic hydrogels. Furthermore, more interventions in the physiological process of hemostasis may provide additional opportunities for the development of functional hemostatic hydrogels.

## Author contributions

Boxiang Zhang: writing – original draft; writing – review and editing; conceptualization; software; and revision of the manuscript; Min Wang: writing – original draft; writing – review and

editing; conceptualization; and revision of the manuscript; Heng Tian: revision of the manuscript; Hang Cai: revision of the manuscript; Siyu Wu: revision of the manuscript; Simin Jiao: revision of the manuscript; Huidong Zhou: revision of the manuscript; Jie Zhao: revision of the manuscript; Yan Li: revision of the manuscript; Wenlai Guo: revision of the manuscript; and Wenrui Qu: revision of the manuscript.

## Conflicts of interest

There are no conflicts to declare.

## Acknowledgements

This work was financed by the Jilin Science and Technology Agency funds in China [grant numbers: 20210101282JC, 20210402001GH, YDZJ202201ZYTS019, YDZJ202201ZYTS572, YDZJ202201ZYTS071 and YDZJ202301ZYTS499], the Jilin Provincial Development and Reform Commission [grant number: 2023C040-2], and the Norman Bethune Project of Jilin University (grant number: 2022B44). We thank Home for Researchers editorial team (<https://www.home-for-researchers.com>) for language editing service.

## References

- B. J. Eastridge, R. L. Mabry, P. Seguin, J. Cantrell, T. Tops, P. Uribe, O. Mallett, T. Zubko, L. Oetjen-Gerdes, T. E. Rasmussen, F. K. Butler, R. S. Kotwal, J. B. Holcomb, C. Wade, H. Champion, M. Lawnick, L. Moores and L. H. Blackbourne, *J. Trauma Acute Care Surg.*, 2012, **73**, S431–S437.
- P. M. Mannucci and M. Levi, *N. Engl. J. Med.*, 2007, **356**, 2301–2311.
- S. A. D. Kyle, J. Kalkwarf, Y. Yang, C. Thetford, L. Myers, M. Brock, D. A. Wolf, D. Persse, C. E. Wade and J. B. Holcomb, *J. Trauma Acute Care Surg.*, 2020, **89**, 716–722.
- B. J. Eastridge, R. L. Mabry, P. Seguin, J. Cantrell, T. Tops, P. Uribe, O. Mallett, T. Zubko, L. Oetjen-Gerdes, T. E. Rasmussen, F. K. Butler, R. S. Kotwal, J. B. Holcomb, C. Wade, H. Champion, M. Lawnick, L. Moores and L. H. Blackbourne, *J. Trauma Acute Care Surg.*, 2012, **73**, S431–S437.
- F. U. R. A. Malik, K. U. Shah, S. S. Naz and S. Qaisar, *J. Biomed. Mater. Res., Part B*, 2021, **109**, 1465–1477.
- P. T. Y. C. H. Tien and F. Brenneman, *Curr. Orthop.*, 2004, **18**, 304–310.
- M. A. Schreiber and B. Tieu, *Surgery*, 2007, **142**, S61–S66.
- B. L. Bennett, *Wilderness Environ. Med.*, 2017, **28**, S39–S49.
- M. Hoekstra, M. Hermans, C. Richters and R. Dutrieux, *J. Wound Care*, 2002, **11**, 113–117.
- M. Xie, Y. Zeng, H. Wu, S. Wang and J. Zhao, *Int. J. Biol. Macromol.*, 2022, **219**, 1337–1350.
- Z. Li and Z. Lin, *Aggregate*, 2021, **2**, 62–87.
- W. Zheng, Z. Zhang, Y. Li, L. Wang, F. Fu, H. Diao and X. Liu, *Chem. Eng. J.*, 2022, **447**, 137482.
- Y.-B. Zhang, H.-J. Wang, A. Raza, C. Liu, J. Yu and J.-Y. Wang, *Int. J. Biol. Macromol.*, 2022, **205**, 110–117.
- J. Tang, W. Yi, J. Yan, Z. Chen, H. Fan, D. Zaldivar-Silva, L. Agüero and S. Wang, *Int. J. Biol. Macromol.*, 2023, **247**, 125754.
- J. Lee, H. N. Choi, H. J. Cha and Y. J. Yang, *Biomacromolecules*, 2023, **24**, 1763–1773.
- Z. Wang, T. Lyu, Q. Xie, Y. Zhang, H. Sun, Y. Wan and Y. Tian, *Appl. Mater. Today*, 2023, **35**, 101948.
- J. Wang, C. Li, W. Zhang, W. Huang, Z. Liu, R. Shi, S. Wang, S. Liu, W. Shi and Y. Li, *Biomater. Sci.*, 2023, **11**, 3616–3628.
- Z. Tan, X. Li, C. Yu, M. Yao, Z. Zhao, B. Guo, L. Liang, Y. Wei, F. Yao and H. Zhang, *Int. J. Biol. Macromol.*, 2023, **232**, 123449.
- Y. Fang, L. Zhang, Y. Chen, S. Wu, Y. Weng and H. Liu, *Carbohydr. Polym.*, 2023, **312**, 120819.
- L. Zheng, Q. Wang, Y. S. Zhang, H. Zhang, Y. Tang, Y. Zhang, W. Zhang and X. Zhang, *Chem. Eng. J.*, 2021, **416**, 129136.
- A. E. Pusateri, J. B. Holcomb, B. S. Kheirabadi, H. B. Alam, C. E. Wade and K. L. Ryan, *J. Trauma Acute Care Surg.*, 2006, **60**, 674–682.
- M. Bahram, N. Mohseni and M. Moghtader, *Emerging concepts in analysis and applications of hydrogels*, IntechOpen, 2016.
- S. Aswathy, U. Narendrakumar and I. Manjubala, *Heliyon*, 2020, **6**, e03719.
- E. M. Ahmed, *J. Adv. Res.*, 2015, **6**, 105–121.
- X. Liu, M. Hou, X. Luo, M. Zheng, X. Wang, H. Zhang and J. Guo, *Biomacromolecules*, 2021, **22**, 319–329.
- C. You, Q. Li, X. Wang, P. Wu, J. K. Ho, R. Jin, L. Zhang, H. Shao and C. Han, *Sci. Rep.*, 2017, **7**, 10489.
- Y. Liang, Z. Li, Y. Huang, R. Yu and B. Guo, *ACS Nano*, 2021, **15**, 7078–7093.
- Q. Tang, C. Chen, Y. Jiang, J. Huang, Y. Liu, P. M. Nthumba, G. Gu, X. Wu, Y. Zhao and J. Ren, *J. Mater. Chem. B*, 2020, **8**, 5756–5764.
- J. Zhu, F. Li, X. Wang, J. Yu and D. Wu, *ACS Appl. Mater. Interfaces*, 2018, **10**, 13304–13316.
- B. J. D. Barba, C. T. Aranilla, L. S. Relleve, V. R. C. Cruz, J. R. Vista and L. V. Abad, *Radiat. Phys. Chem.*, 2018, **144**, 180–188.
- F. Zhou, Y. Yang, W. Zhang, S. Liu, A. B. Shaikh, L. Yang, Y. Lai, H. Ouyang and W. Zhu, *Appl. Mater. Today*, 2022, **26**, 101290.
- L. Teng, Z. Shao, Q. Bai, X. Zhang, Y. S. He, J. Lu, D. Zou, C. Feng and C. M. Dong, *Adv. Funct. Mater.*, 2021, **31**, 2105628.
- C. Y. Zou, X. X. Lei, J. J. Hu, Y. L. Jiang, Q. J. Li, Y. T. Song, Q. Y. Zhang, J. Li-Ling and H. Q. Xie, *Bioact. Mater.*, 2022, **16**, 388–402.
- Q. Zhang, Z. Li, M. Zhang, W. Wang, J. Shen, Z. Ye and N. Zhou, *Langmuir*, 2020, **36**, 13263–13273.
- L. R. Burnett, M. B. Rahmany, J. R. Richter, T. A. Aboushwareb, D. Eberli, C. L. Ward, G. Orlando,



- R. R. Hantgan and M. E. Van Dyke, *Biomaterials*, 2013, **34**, 2632–2640.
- 36 L. Wei, J. Tan, L. Li, H. Wang, S. Liu, J. Chen, Y. Weng and T. Liu, *Int. J. Mol. Sci.*, 2022, **23**, 1249.
- 37 I. Koumentakou, Z. Terzopoulou, A. Michopoulou, I. Kalafatakis, K. Theodorakis, D. Tzetzis and D. Bikiaris, *Int. J. Biol. Macromol.*, 2020, **162**, 693–703.
- 38 J. He, M. Shi, Y. Liang and B. Guo, *Chem. Eng. J.*, 2020, **394**, 124888.
- 39 H. Li, F. Cheng, X. Wei, X. Yi, S. Tang, Z. Wang, Y. S. Zhang, J. He and Y. Huang, *Mater. Sci. Eng., C*, 2021, **118**, 111324.
- 40 M. Suneetha, K. M. Rao and S. S. Han, *ACS Omega*, 2019, **4**, 12647–12656.
- 41 R. Hajosch, M. Suckfuell, S. Oesser, M. Ahlers, K. Flechsenhar and B. Schlosshauer, *J. Biomed. Mater. Res., Part B*, 2010, **94**, 372–379.
- 42 K. Han, Q. Bai, W. Wu, N. Sun, N. Cui and T. Lu, *Int. J. Biol. Macromol.*, 2021, **183**, 2142–2151.
- 43 Y. Chen, Y. Zhang, F. Wang, W. Meng, X. Yang, P. Li, J. Jiang, H. Tan and Y. Zheng, *Mater. Sci. Eng., C*, 2016, **63**, 18–29.
- 44 L. S. Gomez-Aparicio, J. Bernaldez-Sarabia, T. A. Camacho-Villegas, P. H. Lugo-Fabres, N. E. Diaz-Martinez, E. Padilla-Camberos, A. Licea-Navarro and A. B. Castro-Cesena, *Biomater. Sci.*, 2021, **9**, 726–744.
- 45 Z. Yang, X. Fu, L. Zhou, J. Yang, T. Deng, J. Chen, Y. Wen, X. Fu, D. Shen, Z. Yuan, Z. Du, S. Luo and C. Yu, *Chem. Eng. J.*, 2021, **423**, 130202.
- 46 V. Dodane and V. D. Vilivalam, *Pharm. Sci. Technol. Today*, 1998, **1**, 246–253.
- 47 Z. Hu, D.-Y. Zhang, S.-T. Lu, P.-W. Li and S.-D. Li, *Mar. Drugs*, 2018, **16**, 273.
- 48 A. Bal-Ozturk, O. Karal-Yilmaz, Z. P. Akguner, S. Aksu, A. Tas and H. Olmez, *J. Appl. Polym. Sci.*, 2019, **136**, 47522.
- 49 S. Baghaie, M. T. Khorasani, A. Zarrabi and J. Moshtaghian, *J. Biomater. Sci., Polym. Ed.*, 2017, **28**, 2220–2241.
- 50 D. S. Yoon, Y. Lee, H. A. Ryu, Y. Jang, K. M. Lee, Y. Choi, W. J. Choi, M. Lee, K. M. Park, K. D. Park and J. W. Lee, *Acta Biomater.*, 2016, **38**, 59–68.
- 51 H. J. Jang, Y. M. Kim, B. Y. Yoo and Y. K. Seo, *J. Biomater. Appl.*, 2018, **32**, 716–724.
- 52 Z. Ahmadian, A. Correia, M. Hasany, P. Figueiredo, F. Dobakhti, M. R. Eskandari, S. H. Hosseini, R. Abiri, S. Khorshid, J. Hirvonen, H. A. Santos and M. A. Shahbazi, *Adv. Healthcare Mater.*, 2021, **10**, e2001122.
- 53 L. Teng, K. Xia, T. Qian, Z. Hu, L. Hong, Y. Liao, G. Peng, Z. Yuan, Y. Chen and Z. Zeng, *ACS Biomater. Sci. Eng.*, 2022, **8**, 2076–2087.
- 54 C. Xue, H. Xie, J. Eichenbaum, Y. Chen, Y. Wang, F. W. van den Dolder, J. Lee, K. Lee, S. Zhang, W. Sun, A. Sheikhi, S. Ahadian, N. Ashammakhi, M. R. Dokmeci, H. J. Kim and A. Khademhosseini, *Biotechnol. J.*, 2020, **15**, e1900456.
- 55 Y. Huang, B. Zhang, G. Xu and W. Hao, *Compos. Sci. Technol.*, 2013, **84**, 15–22.
- 56 X. Bian, C. Cui, Y. Qi, Y. Sun, Z. Zhang and W. Liu, *Adv. Funct. Mater.*, 2022, **32**, 2207349.
- 57 M. Obst and A. Steinbüchel, *Biomacromolecules*, 2004, **5**, 1166–1176.
- 58 I. Bajaj and R. Singhal, *Bioresour. Technol.*, 2011, **102**, 5551–5561.
- 59 W. Chen, R. Wang, T. Xu, X. Ma, Z. Yao, B. Chi and H. Xu, *J. Mater. Chem. B*, 2017, **5**, 5668–5678.
- 60 W. Chen, S. Yuan, J. Shen, Y. Chen and Y. Xiao, *Front. Bioeng. Biotechnol.*, 2020, **8**, 627351.
- 61 X. Zhang, Z. Ma, Y. Ke, Y. Xia, X. Xu, J. Liu, Y. Gong, Q. Shi and J. Yin, *Mater. Adv.*, 2021, **2**, 5150–5159.
- 62 B. A. Bruckner, L. N. Blau, L. Rodriguez, E. E. Suarez, U. Q. Ngo, M. J. Reardon and M. Loebe, *J. Cardiothorac. Surg.*, 2014, **9**, 134.
- 63 R. Cui, F. Chen, Y. Zhao, W. Huang and C. Liu, *J. Mater. Chem. B*, 2020, **8**, 8282–8293.
- 64 Z. Mirzakhani, K. Faghihi, A. Barati and H. R. Momeni, *Int. J. Polym. Mater. Polym. Biomater.*, 2016, **65**, 779–788.
- 65 J. Drelich, E. Chibowski, D. D. Meng and K. Terpilowski, *Soft Matter*, 2011, **7**, 9804–9828.
- 66 R. Wei, T. Chen, Y. Wang, Q. Xu, B. Feng, J. Weng, W. Peng and J. Wang, *Macromol. Biosci.*, 2021, **21**, e2000367.
- 67 C. Gentilini, Y. Dong, J. R. May, S. Goldoni, D. E. Clarke, B. H. Lee, E. T. Pashuck and M. M. Stevens, *Adv. Healthcare Mater.*, 2012, **1**, 308–315.
- 68 S. Gorgieva and V. Kokol, *Carbohydr. Polym.*, 2011, **85**, 664–673.
- 69 C. Dai, Y. Yuan, C. Liu, J. Wei, H. Hong, X. Li and X. Pan, *Biomaterials*, 2009, **30**, 5364–5375.
- 70 G. Varga, *Epitoanyag*, 2007, **59**, 6–9.
- 71 M. Matsusaki, T. Serizawa, A. Kishida and M. Akashi, *Biomacromolecules*, 2005, **6**, 400–407.
- 72 T.-Y. Liu, S.-Y. Chen, Y.-L. Lin and D.-M. Liu, *Langmuir*, 2006, **22**, 9740–9745.
- 73 L. Shen, Y. Zhang, W. Yu, R. Li, M. Wang, Q. Gao, J. Li and H. Lin, *J. Colloid Interface Sci.*, 2019, **543**, 64–75.
- 74 T. Coviello, P. Matricardi, C. Marianecchi and F. Alhaique, *J. Controlled Release*, 2007, **119**, 5–24.
- 75 J. Alam, M. Alhoshan, A. K. Shukla, A. Aldalbahi and F. A. A. Ali, *Eur. Polym. J.*, 2019, **120**, 109219.
- 76 B. J. D. Barba, C. Tranquilar-Aranilla and L. V. Abad, *Radiat. Phys. Chem.*, 2016, **118**, 111–113.
- 77 X. Luo, F. Ao, Q. Huo, Y. Liu, X. Wang, H. Zhang, M. Yang, Y. Ma and X. Liu, *Biomater. Adv.*, 2022, **139**, 212983.
- 78 H. F. Liu, J. S. Mao, K. D. Yao, G. H. Yang, L. Cui and Y. L. Cao, *J. Biomater. Sci., Polym. Ed.*, 2004, **15**, 25–40.
- 79 A. Z. Bazmandeh, E. Mirzaei, M. Fadaie, S. Shirian and Y. Ghasemi, *Int. J. Biol. Macromol.*, 2020, **162**, 359–373.
- 80 Y. Wang, R. Fu, X. Ma, X. Li and D. Fan, *Macromol. Biosci.*, 2021, **21**, e2000396.
- 81 C. Wang, H. Niu, X. Ma, H. Hong, Y. Yuan and C. Liu, *ACS Appl. Mater. Interfaces*, 2019, **11**, 34595–34608.
- 82 E. D. Bain, T. R. Long, F. L. Beyer, A. M. Savage, M. D. Dadmun, H. Martin, J. L. Lenhart and R. A. Mrozek, *Macromolecules*, 2018, **51**, 4705–4717.
- 83 Y. Liu, H. Meng, S. Konst, R. Sarmiento, R. Rajachar and B. P. Lee, *ACS Appl. Mater. Interfaces*, 2014, **6**, 16982–16992.



- 84 T. Sakai, T. Matsunaga, Y. Yamamoto, C. Ito, R. Yoshida, S. Suzuki, N. Sasaki, M. Shibayama and U.-I. Chung, *Macromolecules*, 2008, **41**, 5379–5384.
- 85 Y. Bu, L. Zhang, J. Liu, L. Zhang, T. Li, H. Shen, X. Wang, F. Yang, P. Tang and D. Wu, *ACS Appl. Mater. Interfaces*, 2016, **8**, 12674–12683.
- 86 H. Yuk, T. Zhang, G. A. Parada, X. Liu and X. Zhao, *Nat. Commun.*, 2016, **7**, 12028.
- 87 H. Pan, D. Fan, W. Cao, C. Zhu, Z. Duan, R. Fu, X. Li and X. Ma, *Polymers*, 2017, **9**, 727.
- 88 T. M. Tamer, M. M. Sabet, A. M. Omer, E. Abbas, A. I. Eid, M. S. Mohy-Eldin and M. A. Hassan, *Sci. Rep.*, 2021, **11**, 3428.
- 89 C. Wang, H. Guo, S. Leng, J. Yu, K. Feng, L. Cao and J. Huang, *Crit. Rev. Solid State Mater. Sci.*, 2021, **46**, 330–348.
- 90 X. Shang, H. Chen, V. Castagnola, K. Liu, L. Boselli, V. Petseva, L. Yu, L. Xiao, M. He and F. Wang, *Nat. Catal.*, 2021, **4**, 607–614.
- 91 F. Arnaud, T. Tomori, W. Carr, A. McKeague, K. Teranishi, K. Prusaczyk and R. McCarron, *Ann. Biomed. Eng.*, 2008, **36**, 1708–1713.
- 92 L. Yu, X. Shang, H. Chen, L. Xiao, Y. Zhu and J. Fan, *Nat. Commun.*, 2019, **10**, 1932.
- 93 P. Fathi, M. Sikorski, K. Christodoulides, K. Langan, Y. S. Choi, M. Titcomb, A. Ghodasara, O. Wonodi, H. Thaker, M. Vural, A. Behrens and P. Kofinas, *J. Biomed. Mater. Res., Part B*, 2018, **106**, 1662–1671.
- 94 T. Zhu, J. Wu, N. Zhao, C. Cai, Z. Qian, F. Si, H. Luo, J. Guo, X. Lai, L. Shao and J. Xu, *Adv. Healthcare Mater.*, 2018, **7**, e1701086.
- 95 Z. Li, A. Millionis, Y. Zheng, M. Yee, L. Codispoti, F. Tan, D. Poulidakos and C. H. Yap, *Nat. Commun.*, 2019, **10**, 5562.
- 96 J. C. Lantis, F. M. Durville, R. Connolly and S. D. Schwaitzberg, *J. Laparoendosc. Adv. Surg. Tech., Part A*, 1998, **8**, 381–394.
- 97 L. Li, B. Yan, J. Yang, L. Chen and H. Zeng, *Adv. Mater.*, 2015, **27**, 1294–1299.
- 98 W. Han and S. Wang, *Gels*, 2022, **9**, 2.
- 99 X. B. Zhang, L. X. Shi, W. Y. Xiao, Z. Wang and S. T. Wang, *Adv. Nanobiomed. Res.*, 2023, **3**, 2200115.
- 100 X. Xia, X. Xu, B. Wang, D. Zhou, W. Zhang, X. Xie, H. Lai, J. Xue, A. Rai, Z. Li, X. Peng, P. Zhao, L. Bian and P. W. Y. Chiu, *Adv. Funct. Mater.*, 2022, **32**, 2109332.
- 101 S. Komatsu, Y. Nagai, K. Naruse and Y. Kimata, *PLoS One*, 2014, **9**, e102778.
- 102 C. Ding, M. Tian, R. Feng, Y. Dang and M. Zhang, *ACS Biomater. Sci. Eng.*, 2020, **6**, 3855–3867.
- 103 H. Li, X. Zhou, L. Luo, Q. Ding and S. Tang, *Carbohydr. Polym.*, 2022, **281**, 119039.
- 104 P. Ni, S. Ye, S. Xiong, M. Zhong, J. Shan, T. Yuan, J. Liang, Y. Fan and X. Zhang, *J. Mater. Chem. B*, 2023, **11**, 5207–5222.
- 105 X.-X. Lei, J.-J. Hu, C.-Y. Zou, Y.-L. Jiang, L.-M. Zhao, X.-Z. Zhang, Y.-X. Li, A.-N. Peng, Y.-T. Song and L.-P. Huang, *Bioact. Mater.*, 2023, **27**, 461–473.
- 106 M. F.-H. Lee and A. Ananda, *Auris Nasus Larynx*, 2023, **50**, 365–373.
- 107 K. Zhang, X. Chen, Y. Xue, J. Lin, X. Liang, J. Zhang, J. Zhang, G. Chen, C. Cai and J. Liu, *Adv. Funct. Mater.*, 2021, **32**, 2111465.
- 108 S. Bai, X. Zhang, P. Cai, X. Huang, Y. Huang, R. Liu, M. Zhang, J. Song, X. Chen and H. Yang, *Nanoscale Horiz.*, 2019, **4**, 1333–1341.
- 109 R. Mrówczyński, R. Markiewicz and J. Liebscher, *Polym. Int.*, 2016, **65**, 1288–1299.
- 110 Z. Guo, W. Xie, J. Lu, X. Guo, J. Xu, W. Xu, Y. Chi, N. Takuya, H. Wu and L. Zhao, *J. Mater. Chem. B*, 2021, **9**, 4098–4110.
- 111 Y.-G. Jang, E.-B. Ko and K.-C. Choi, *J. Nutr. Biochem.*, 2020, **84**, 108444.
- 112 M. Shin, J. H. Ryu, J. P. Park, K. Kim, J. W. Yang and H. Lee, *Adv. Funct. Mater.*, 2015, **25**, 1270–1278.
- 113 Y. N. Chen, L. Peng, T. Liu, Y. Wang, S. Shi and H. Wang, *ACS Appl. Mater. Interfaces*, 2016, **8**, 27199–27206.
- 114 Y. Yang, X. Zhao, J. Yu, X. Chen, R. Wang, M. Zhang, Q. Zhang, Y. Zhang, S. Wang and Y. Cheng, *Bioact. Mater.*, 2021, **6**, 3962–3975.
- 115 X. H. Shao, X. Yang, Y. Zhou, Q. C. Xia, Y. P. Lu, X. Yan, C. Chen, T. T. Zheng, L. L. Zhang, Y. N. Ma, Y. X. Ma and S. Z. Gao, *Soft Matter*, 2022, **18**, 2814–2828.
- 116 L. Wang, X. Zhang, K. Yang, Y. V. Fu, T. Xu, S. Li, D. Zhang, L. N. Wang and C. S. Lee, *Adv. Funct. Mater.*, 2019, **30**, 1904156.
- 117 J. Guo, H. Sun, K. Alt, B. L. Tardy, J. J. Richardson, T. Suma, H. Ejima, J. Cui, C. E. Hagemeyer and F. Caruso, *Adv. Healthcare Mater.*, 2015, **4**, 1796–1801.
- 118 S. M. Kang, N. S. Hwang, J. Yeom, S. Y. Park, P. B. Messersmith, I. S. Choi, R. Langer, D. G. Anderson and H. Lee, *Adv. Funct. Mater.*, 2012, **22**, 2949–2955.
- 119 S. Lamping, T. Otremba and B. J. Ravoo, *Angew. Chem., Int. Ed.*, 2018, **57**, 2474–2478.
- 120 P. Deng, X. Liang, F. Chen, Y. Chen and J. Zhou, *Appl. Mater. Today*, 2022, **26**, 101362.
- 121 W. Huang, Y. Wang, Y. Chen, Y. Zhao, Q. Zhang, X. Zheng, L. Chen and L. Zhang, *Adv. Healthcare Mater.*, 2016, **5**, 2813–2822.
- 122 W. Fang, L. Yang, L. Hong and Q. Hu, *Carbohydr. Polym.*, 2021, **271**, 118428.
- 123 J. Saiz-Poseu, J. Mancebo-Aracil, F. Nador, F. Busqué and D. Ruiz-Molina, *Angew. Chem., Int. Ed.*, 2019, **58**, 696–714.
- 124 M. Xie, Z. Zheng, S. Pu, Y. G. Jia, L. Wang and Y. Chen, *Macromol. Biosci.*, 2022, **22**, e2100491.
- 125 S. Yan, W. Wang, X. Li, J. Ren, W. Yun, K. Zhang, G. Li and J. Yin, *J. Mater. Chem. B*, 2018, **6**, 6377–6390.
- 126 Y. Liang, X. Zhao, T. Hu, B. Chen, Z. Yin, P. X. Ma and B. Guo, *Small*, 2019, **15**, e1900046.
- 127 D. Wang, P. Xu, S. Wang, W. Li and W. Liu, *Eur. Polym. J.*, 2020, **134**, 109763.
- 128 J. Hoque, R. G. Prakash, K. Paramanandham, B. R. Shome and J. Halder, *Mol. Pharmaceutics*, 2017, **14**, 1218–1230.
- 129 M. B. Dowling, R. Kumar, M. A. Keibler, J. R. Hess, G. V. Bochicchio and S. R. Raghavan, *Biomaterials*, 2011, **32**, 3351–3357.



- 130 J. Qu, X. Zhao, Y. Liang, T. Zhang, P. X. Ma and B. Guo, *Biomaterials*, 2018, **183**, 185–199.
- 131 X. Wei, C. Cui, C. Fan, T. Wu, Y. Li, X. Zhang, K. Wang, Y. Pang, P. Yao and J. Yang, *Int. J. Biol. Macromol.*, 2022, **199**, 401–412.
- 132 Y. Xiong, L. Chen, P. Liu, T. Yu, C. Lin, C. Yan, Y. Hu, W. Zhou, Y. Sun, A. C. Panayi, F. Cao, H. Xue, L. Hu, Z. Lin, X. Xie, X. Xiao, Q. Feng, B. Mi and G. Liu, *Small*, 2022, **18**, e2104229.
- 133 H. Zhu, X. Mei, Y. He, H. Mao, W. Tang, R. Liu, J. Yang, K. Luo, Z. Gu and L. Zhou, *ACS Appl. Mater. Interfaces*, 2020, **12**, 4241–4253.
- 134 D. S. Hwang, H. Zeng, Q. Lu, J. Israelachvili and J. H. Waite, *Soft Matter*, 2012, **8**, 5640–5648.
- 135 T. Thiruselvi, S. Thirupathi Kumara Raja, R. Aravindhan, S. K. Shanuja and A. Gnanamani, *RSC Adv.*, 2016, **6**, 19973–19981.
- 136 M. Zhang, J. Yu, K. Shen, R. Wang, J. Du, X. Zhao, Y. Yang, K. Xu, Q. Zhang, Y. Zhang and Y. Cheng, *Chem. Mater.*, 2021, **33**, 6453–6463.
- 137 H. Weng, W. Jia, M. Li and Z. Chen, *Carbohydr. Polym.*, 2022, **294**, 119767.
- 138 W. Qiu, H. Han, M. Li, N. Li, Q. Wang, X. Qin, X. Wang, J. Yu, Y. Li and F. Li, *J. Colloid Interface Sci.*, 2021, **596**, 312–323.
- 139 Y. Deng, J. Chen, J. Huang, X. Yang, X. Zhang, S. Yuan and W. Liao, *Cellulose*, 2020, **27**, 3971–3988.
- 140 J. W. Luo, C. Liu, J. H. Wu, L. X. Lin, H. M. Fan, D. H. Zhao, Y. Q. Zhuang and Y. L. Sun, *Mater. Sci. Eng., C*, 2019, **98**, 628–634.
- 141 Z. Mirzakhani, K. Faghihi, A. Barati and H. R. Momeni, *J. Biomater. Sci., Polym. Ed.*, 2015, **26**, 1439–1451.
- 142 J. Yu, X. Li, N. Chen, S. Xue, J. Zhao, S. Li, X. Hou and X. Yuan, *Colloids Surf., B*, 2022, **215**, 112508.
- 143 J. Liu, J. Li, F. Yu, Y. X. Zhao, X. M. Mo and J. F. Pan, *Int. J. Biol. Macromol.*, 2020, **147**, 653–666.
- 144 K. Fujii, H. Asai, T. Ueki, T. Sakai, S. Imaizumi, U.-I. Chung, M. Watanabe and M. Shibayama, *Soft Matter*, 2012, **8**, 1756–1759.
- 145 Y. Kong, Z. Hou, L. Zhou, P. Zhang, Y. Ouyang, P. Wang, Y. Chen and X. Luo, *ACS Biomater. Sci. Eng.*, 2021, **7**, 335–349.
- 146 A. Ovsianikov, M. Malinauskas, S. Schlie, B. Chichkov, S. Gittard, R. Narayan, M. Löbner, K. Sternberg, K.-P. Schmitz and A. Haverich, *Acta Biomater.*, 2011, **7**, 967–974.
- 147 M. Rodrigues, N. Kosaric, C. A. Bonham and G. C. Gurtner, *Physiol. Rev.*, 2019, **99**, 665–706.
- 148 D. A. Triplett, *Clin. Chem.*, 2000, **46**, 1260–1269.
- 149 S. Palta, R. Saroa and A. Palta, *Indian J. Anaesth.*, 2014, **58**, 515–523.
- 150 M. McMichael, *J. Vet. Emerg. Crit. Care*, 2005, **15**, 1–8.
- 151 K. Broos, H. B. Feys, S. F. De Meyer, K. Vanhoorelbeke and H. Deckmyn, *Blood Rev.*, 2011, **25**, 155–167.
- 152 H. H. Versteeg, J. W. Heemskerk, M. Levi and P. H. Reitsma, *Physiol. Rev.*, 2013, **93**, 327–358.
- 153 J. M. Stassen, J. Arnout and H. Deckmyn, *Curr. Med. Chem.*, 2004, **11**, 2245–2260.
- 154 J. W. Weisel, *Adv. Protein Chem.*, 2005, **70**, 247–299.
- 155 E. Di Cera, *Mol. Aspects Med.*, 2008, **29**, 203–254.
- 156 J. W. Weisel and R. I. Litvinov, *Fibrous Proteins*, 2017, 405–456.
- 157 D. Lasne, B. Jude and S. Susen, *Can. J. Anaesth.*, 2006, **53**, S2–S11.
- 158 A. T. Franco, A. Corken and J. Ware, *Blood*, 2015, **126**, 582–588.
- 159 B. Estevez and X. Du, *Physiology*, 2017, **32**, 162–177.
- 160 H. Zheng, S. Wang, F. Cheng, X. He, Z. Liu, W. Wang, L. Zhou and Q. Zhang, *Chem. Eng. J.*, 2021, **424**, 130148.
- 161 D. Zhang, Z. Xu, H. Li, C. Fan, C. Cui, T. Wu, M. Xiao, Y. Yang, J. Yang and W. Liu, *Biomater. Sci.*, 2020, **8**, 1455–1463.
- 162 N. Zandi, B. Dolatyar, R. Lotfi, Y. Shallageh, M. A. Shokrgozar, E. Tamjid, N. Annabi and A. Simchi, *Acta Biomater.*, 2021, **124**, 191–204.
- 163 S. A. Santoro, *Cell*, 1986, **46**, 913–920.
- 164 I. D. Campbell and M. J. Humphries, *Cold Spring Harbor Perspect. Biol.*, 2011, **3**, a004994.
- 165 J.-f Dong, J. L. Moake, L. Nolasco, A. Bernardo, W. Arceneaux, C. N. Shrimpton, A. J. Schade, L. V. McIntire, K. Fujikawa and J. A. López, *Blood, J. Am. Soc. Hematol.*, 2002, **100**, 4033–4039.
- 166 T. A. Springer, *Blood*, 2014, **124**, 1412–1425.
- 167 R. K. Andrews and M. C. Berndt, *Thromb. Res.*, 2004, **114**, 447–453.
- 168 W. Zhang, W. Deng, L. Zhou, Y. Xu, W. Yang, X. Liang, Y. Wang, J. D. Kulman, X. F. Zhang and R. Li, *Blood, J. Am. Soc. Hematol.*, 2015, **125**, 562–569.
- 169 Z. M. Ruggeri, *Blood, J. Am. Soc. Hematol.*, 2015, **125**, 423–424.
- 170 E. M. Golebiewska and A. W. Poole, *Blood Rev.*, 2015, **29**, 153–162.
- 171 M. D. Linden, *Methods Mol. Biol.*, 2013, **992**, 13–30.
- 172 T. Gremmel, A. L. Frelinger, 3rd and A. D. Michelson, *Semin. Thromb. Haemostasis*, 2016, **42**, 191–204.
- 173 R. Liu, L. Dai, C. Si and Z. Zeng, *Carbohydr. Polym.*, 2018, **195**, 63–70.
- 174 Y. Liu, H. Niu, C. Wang, X. Yang, W. Li, Y. Zhang, X. Ma, Y. Xu, P. Zheng, J. Wang and K. Dai, *Bioact. Mater.*, 2022, **17**, 162–177.
- 175 K. Zheng, Y. Tong, S. Zhang, R. He, L. Xiao, Z. Iqbal, Y. Zhang, J. Gao, L. Zhang, L. Jiang and Y. Li, *Adv. Funct. Mater.*, 2021, **31**, 2102599.
- 176 N. D. Sanandhiya, S. Lee, S. Rho, H. Lee, I. S. Kim and D. S. Hwang, *Carbohydr. Polym.*, 2019, **208**, 77–85.
- 177 A. Radomski, P. Jurasz, D. Alonso-Escolano, M. Drews, M. Morandi, T. Malinski and M. W. Radomski, *Br. J. Pharmacol.*, 2005, **146**, 882–893.
- 178 A. K. Gaharwar, R. K. Avery, A. Assmann, A. Paul, G. H. McKinley, A. Khademhosseini and B. D. Olsen, *ACS Nano*, 2014, **8**, 9833–9842.
- 179 P. Roach, D. Farrar and C. C. Perry, *J. Am. Chem. Soc.*, 2005, **127**, 8168–8173.
- 180 M. H. Kim, J. Lee, J. N. Lee, H. Lee and W. H. Park, *Acta Biomater.*, 2021, **123**, 254–262.



- 181 S. Atefyekta, E. Blomstrand, A. K. Rajasekharan, S. Svensson, M. Trobos, J. Hong, T. J. Webster, P. Thomsen and M. Andersson, *ACS Biomater. Sci. Eng.*, 2021, **7**, 1693–1702.
- 182 Z. Zhai, K. Xu, L. Mei, C. Wu, J. Liu, Z. Liu, L. Wan and W. Zhong, *Soft Matter*, 2019, **15**, 8603–8610.
- 183 M. Zhang, D. Wang, N. Ji, S. Lee, G. Wang, Y. Zheng, X. Zhang, L. Yang, Z. Qin and Y. Yang, *Polymers*, 2021, **13**, 199–209.
- 184 R. Hao, X. Peng, Y. Zhang, J. Chen, T. Wang, W. Wang, Y. Zhao, X. Fan, C. Chen and H. Xu, *ACS Appl. Mater. Interfaces*, 2020, **12**, 55574–55583.
- 185 S. Wang, X. Ji, S. Chen, C. Zhang, Y. Wang, H. Lin and L. Zhao, *Eur. Polym. J.*, 2022, **162**, 110875.
- 186 X. Chen, C. Cui, Y. Liu, C. Fan, M. Xiao, D. Zhang, Z. Xu, Y. Li, J. Yang and W. Liu, *Biomater. Sci.*, 2020, **8**, 3760–3771.
- 187 G. Chen, Y. Yu, X. Wu, G. Wang, J. Ren and Y. Zhao, *Adv. Funct. Mater.*, 2018, **28**, 1801386.
- 188 M. B. Rahmany, R. R. Hantgan and M. Van Dyke, *Biomaterials*, 2013, **34**, 2492–2500.
- 189 D. Wang, W. Li, Y. Wang, H. Yin, Y. Ding, J. Ji, B. Wang and S. Hao, *Colloids Surf., B*, 2019, **182**, 110367.
- 190 A. Tang, Y. Li, Y. Yao, X. Yang, Z. Cao, H. Nie and G. Yang, *Biomater. Sci.*, 2021, **9**, 4169–4177.
- 191 Z. Sun, X. Chen, X. Ma, X. Cui, Z. Yi and X. Li, *J. Mater. Chem. B*, 2018, **6**, 6133–6141.
- 192 E. J. Kim, J. S. Choi, J. S. Kim, Y. C. Choi and Y. W. Cho, *Biomacromolecules*, 2016, **17**, 4–11.
- 193 R. D. Ventura, A. R. Padalhin and B. T. Lee, *Mater. Lett.*, 2018, **232**, 130–133.
- 194 S. Shen, D. Fan, Y. Yuan, X. Ma, J. Zhao and J. Yang, *Chem. Eng. J.*, 2021, **426**, 130610.
- 195 Y. Yuan, D. Fan, S. Shen and X. Ma, *Chem. Eng. J.*, 2022, **433**, 133859.
- 196 J. W. Weisel and R. I. Litvinov, *J. Thromb. Haemostasis*, 2019, **17**, 271–282.
- 197 R. Marchioli, G. Finazzi, G. Specchia, R. Cacciola, R. Cavazzina, D. Cillonì, V. De Stefano, E. Elli, A. Iurlo and R. Latagliata, *N. Engl. J. Med.*, 2013, **368**, 22–33.
- 198 V. X. Du, D. Huskens, C. Maas, R. Al Dieri, P. G. de Groot and B. de Laat, *Semin. Thromb. Hemostasis*, 2014, **40**, 72–80.
- 199 C. Klatt, I. Krüger, S. Zey, K.-J. Krott, M. Spelleken, N. S. Gowert, A. Oberhuber, L. Pfaff, W. Lückstädt and K. Jurk, *J. Clin. Invest.*, 2018, **128**, 3906–3925.
- 200 M. Spengler, M. Svetaz, M. Leroux, S. Bertoluzzo, P. Carrara, F. Van Isseldyk, D. Petrelli, F. Parente and P. Bosch, *Clin. Hemorheol. Microcirc.*, 2011, **47**, 279–285.
- 201 E. B. Assayag, N. Bornstein, I. Shapira, T. Mardi, Y. Goldin, T. Tolshinski, Y. Vered, V. Zakuth, M. Burke and S. Berliner, *Int. J. Cardiol.*, 2005, **98**, 271–276.
- 202 K. C. Gersh, C. Nagaswami and J. W. Weisel, *J. Thromb. Haemostasis*, 2009, **102**, 1169–1175.
- 203 J. Weisel and R. Litvinov, *J. Thromb. Haemostasis*, 2019, **17**, 271–282.
- 204 G. Barshtein, R. Ben-Ami and S. Yedgar, *Expert Rev. Cardiovasc. Ther.*, 2007, **5**, 743–752.
- 205 M. Wang, J. Hu, Y. Ou, X. He, Y. Wang, C. Zou, Y. Jiang, F. Luo, D. Lu, Z. Li, J. Li and H. Tan, *ACS Appl. Mater. Interfaces*, 2022, **14**, 17093–17108.
- 206 M. Kedzierska, S. Blilid, K. Milowska, J. Kolodziejczyk-Czepas, N. Katir, M. Lahcini, A. El Kadib and M. Bryszewska, *Int. J. Mol. Sci.*, 2021, **22**, 11386.
- 207 N. Mackman, *Anesth. Analg.*, 2009, **108**, 1447.
- 208 S. P. Grover and N. Mackman, *Arterioscler., Thromb., Vasc. Biol.*, 2019, **39**, 331–338.
- 209 P. E. van der Meijden, I. C. Munnix, J. M. Auger, J. W. Govers-Riemslog, J. M. Cosemans, M. J. Kuijpers, H. M. Spronk, S. P. Watson, T. Renné and J. W. Heemskerk, *Blood, J. Am. Soc. Hematol.*, 2009, **114**, 881–890.
- 210 M. Didiasova, L. Wujak, L. Schaefer and M. Wygrecka, *Cell. Signal.*, 2018, **51**, 257–265.
- 211 S. P. Grover and N. Mackman, *Arterioscler., Thromb., Vasc. Biol.*, 2018, **38**, 709–725.
- 212 N. Mackman, R. E. Tilley and N. S. Key, *Arterioscler., Thromb., Vasc. Biol.*, 2007, **27**, 1687–1693.
- 213 L. Zhang, Y. Zhang, F. Ma, X. Liu, Y. Liu, Y. Cao and R. Pei, *J. Mater. Chem. B*, 2022, **10**, 915–926.
- 214 Z. Chen, D. Fan and L. Shang, *Biomed. Mater.*, 2020, **16**, 012001.
- 215 S. Gao, L. Qu, C. Zhu, P. Ouyang and D. Fan, *Sci. China: Technol. Sci.*, 2020, **63**, 2449–2463.
- 216 S. Tavakoli, M. Kharaziha, S. Nemati and A. Kalateh, *Carbohydr. Polym.*, 2021, **251**, 117013.
- 217 N. Golafshan, R. Rezaheh, M. Tarkesh Esfahani, M. Kharaziha and S. N. Khorasani, *Carbohydr. Polym.*, 2017, **176**, 392–401.
- 218 A. Basu, J. Hong and N. Ferraz, *Macromol. Biosci.*, 2017, **17**, 1700236.
- 219 X. Fan, S. Wang, Y. Fang, P. Li, W. Zhou, Z. Wang, M. Chen and H. Liu, *Mater. Sci. Eng., C*, 2020, **109**, 110649.
- 220 D. Green, *Hemodialysis Int.*, 2006, **10**, S2–S4.
- 221 T. Subramaniam, M. B. Fauzi, Y. Lokanathan and J. X. Law, *Int. J. Mol. Sci.*, 2021, **22**, 6486.
- 222 H. Cheng, W. Shi, L. Feng, J. Bao, Q. Chen, W. Zhao and C. Zhao, *J. Mater. Chem. B*, 2021, **9**, 6678–6690.
- 223 F. Risser, I. Urosev, J. Lopez-Morales, Y. Sun and M. A. Nash, *Biophys. Rev.*, 2022, 1–35, DOI: [10.1007/s12551-022-00950-w](https://doi.org/10.1007/s12551-022-00950-w).
- 224 N. J. Mutch, *Blood*, 2019, **134**, SCI-18.
- 225 S. Bru, J. M. Martínez-Laínez, S. Hernández-Ortega, E. Quandt, J. Torres-Torronteras, R. Martí, D. Canadell, J. Ariño, S. Sharma, J. Jiménez and J. Clotet, *Mol. Microbiol.*, 2016, **101**, 367–380.
- 226 S. H. Choi, S. A. Smith and J. H. Morrissey, *Blood*, 2011, **118**, 6963–6970.
- 227 S. A. Smith, S. H. Choi, R. Davis-Harrison, J. Huyck, J. Boettcher, C. M. Rienstra and J. H. Morrissey, *Blood*, 2010, **116**, 4353–4359.
- 228 J. L. Mitchell, A. S. Lionikiene, G. Georgiev, A. Klemmer, C. Brain, P. Y. Kim and N. J. Mutch, *Blood*, 2016, **128**, 2834–2845.
- 229 D. Chen, X. Liu, Y. Qi, X. Ma, Y. Wang, H. Song, Y. Zhao, W. Li and J. Qin, *Colloids Surf., B*, 2022, **214**, 112430.



- 230 D. Chen, X. Zhou, L. Chang, Y. Wang, W. Li and J. Qin, *Biomacromolecules*, 2021, **22**, 2272–2283.
- 231 M. Sakoda, M. Kaneko, S. Ohta, P. Qi, S. Ichimura, Y. Yatomi and T. Ito, *Biomacromolecules*, 2018, **19**, 3280–3290.
- 232 C. Cao, N. Yang, Y. Zhao, D. Yang, Y. Hu, D. Yang, X. Song, W. Wang and X. Dong, *Nano Today*, 2021, **39**, 101165.
- 233 H. Stoll, H. Steinle, K. Stang, S. Kunnakattu, L. Scheideler, B. Neumann, J. Kurz, I. Degenkolbe, N. Perle, C. Schlensak, H. P. Wendel and M. Avci-Adali, *Macromol. Biosci.*, 2017, **17**, 1600252.
- 234 S. Charbonneau, C. A. Lemarie, H. T. Peng, J. G. Ganopolsky, P. N. Shek and M. D. Blostein, *J. Trauma Acute Care Surg.*, 2012, **72**, 136–142.
- 235 D. Zhang, Z. Hu, L. Zhang, S. Lu, F. Liang and S. Li, *Materials*, 2020, **13**, 5038.
- 236 J. Zhu, H. Han, F. Li, X. Wang, J. Yu, X. Qin and D. Wu, *Chem. Mater.*, 2019, **31**, 4436–4450.
- 237 Y. Ouyang, Y. Zhao, X. Zheng, Y. Zhang, J. Zhao, S. Wang and Y. Gu, *Int. J. Biol. Macromol.*, 2023, **242**, 124960.
- 238 Q. Zhou, X. Zhou, Z. Mo, Z. Zeng, Z. Wang, Z. Cai, L. Luo, Q. Ding, H. Li and S. Tang, *Int. J. Biol. Macromol.*, 2023, **224**, 370–379.
- 239 E. Khadem, M. Kharaziha and S. Salehi, *Mater. Today Bio.*, 2023, **20**, 100650.
- 240 N. Zhang, X. Zhang, Y. Zhu, D. Wang, R. Li, S. Li, R. Meng, Z. Liu and D. Chen, *Polymers*, 2023, **15**, 4362.
- 241 Z. Chen, J. Yao, J. Zhao and S. Wang, *Int. J. Biol. Macromol.*, 2023, **225**, 1235–1245.
- 242 S. Xu, J. You, S. Yan, L. Zhu and X. Wu, *J. Mater. Chem. B*, 2023, **11**, 9950–9960.
- 243 H. Song, L. Xing, W. Liu, X. Wang, Z. Hou, Y. Wang, Z. Zhang, Y. Li, T. Li, X. Wang, H. Chen, S. Xing and J. Xu, *Biomacromolecules*, 2023, **24**, 3327–3344.
- 244 Z. Chen, J. Zhao, H. Wu, H. Wang, X. Lu, M.-A. Shahbazi and S. Wang, *Carbohydr. Polym.*, 2023, **303**, 120434.
- 245 M. Suneetha, S. Zo, S. M. Choi and S. S. Han, *Int. J. Biol. Macromol.*, 2023, **241**, 124641.
- 246 P. Fan, Q. Dong, J. Yang, Y. Chen, H. Yang, S. Gu, W. Xu and Y. Zhou, *Carbohydr. Polym.*, 2023, **313**, 120854.
- 247 D. Zhang, L. Mei, Y. Hao, B. Yi, J. Hu, D. Wang, Y. Zhao, Z. Wang, H. Huang and Y. Xu, *Biomater. Res.*, 2023, **27**, 1–15.
- 248 A. Osman, E. Lin and D. S. Hwang, *Carbohydr. Polym.*, 2023, **299**, 120172.
- 249 H. Wang, J. Cheng, F. Sun, X. Dou, J. Liu, Y. Wang, M. Li, J. Gao, X. Liu and X. Wang, *Adv. Mater.*, 2023, **35**, 2208622.
- 250 R. Haghniaz, H. Montazerian, A. Rabbani, A. Baidya, B. Usui, Y. Zhu, M. Tavafoghi, F. Wahid, H. J. Kim and A. Sheikhi, *Adv. Healthcare Mater.*, 2023, 2301551.
- 251 C. Liu, C. Liu, Z. Liu, Z. Shi, S. Liu, X. Wang, X. Wang and F. Huang, *Int. J. Biol. Macromol.*, 2023, **224**, 1091–1100.
- 252 H. Cheng, Q. Yu, Q. Chen, L. Feng, W. Zhao and C. Zhao, *Biomater. Sci.*, 2023, **11**, 931–948.
- 253 W. Fang, L. Yang, Y. Chen and Q. Hu, *Acta Biomater.*, 2023, **161**, 50–66.
- 254 M. Mecwan, R. Haghniaz, A. H. Najafabadi, K. Mandal, V. Jucaud, J. V. John and A. Khademhosseini, *Biomater. Sci.*, 2023, **11**, 949–963.
- 255 N. Wang, K. Yu, K. Li and X. Yu, *J. Mater. Chem. B*, 2023, **11**, 1232–1239.
- 256 Z. Xu, T. Chen, K. Q. Zhang, K. Meng and H. Zhao, *Polym. Int.*, 2021, **70**, 1741–1751.
- 257 Y. Yuan, S. Shen and D. Fan, *Biomaterials*, 2021, **276**, 120838.
- 258 I. A. Duceac, L. Verestiuc, C. D. Dimitriu, V. Maier and S. Coseri, *Polymers*, 2020, **12**, 1473.
- 259 L. Fan, H. Yang, J. Yang, M. Peng and J. Hu, *Carbohydr. Polym.*, 2016, **146**, 427–434.
- 260 C. Guo, Y. Wu, W. Li, Y. Wang and Q. Kong, *ACS Appl. Mater. Interfaces*, 2022, **14**, 30480–30492.
- 261 Y. Wang, Y. Wu, L. Long, L. Yang, D. Fu, C. Hu, Q. Kong and Y. Wang, *ACS Appl. Mater. Interfaces*, 2021, **13**, 33584–33599.
- 262 X. Zhang, G. H. Sun, M. P. Tian, Y. N. Wang, C. C. Qu, X. J. Cheng, C. Feng and X. G. Chen, *Int. J. Biol. Macromol.*, 2019, **138**, 321–333.
- 263 Q. Bai, L. Teng, X. Zhang and C. M. Dong, *Adv. Healthcare Mater.*, 2022, **11**, e2101809.
- 264 D. Cai, S. Chen, B. Wu, J. Chen, D. Tao, Z. Li, Q. Dong, Y. Zou, Y. Chen, C. Bi, D. Zu, L. Lu and B. Fang, *Mater. Today Bio.*, 2021, **12**, 100127.
- 265 J. Chen, J. He, Y. Yang, L. Qiao, J. Hu, J. Zhang and B. Guo, *Acta Biomater.*, 2022, **146**, 119–130.
- 266 T. Zhang, J. Zhao, X. Lv, F. Liu, X. Wang, K. Li, Z. Bai, H. Chen and W. Tian, *J. Nanopart. Res.*, 2021, **23**, 240.
- 267 O. Goncharuk, O. Korotych, Y. Samchenko, L. Kernosenko, A. Kravchenko, L. Shtanova, C. U. C. O. Tssmall, T. Poltoratska, N. Pasmurtseva, I. Mamyshev, E. Pakhlov and O. Siryk, *Mater. Sci. Eng., C*, 2021, **129**, 112363.
- 268 X. Zhao, Y. Liang, Y. Huang, J. He, Y. Han and B. Guo, *Adv. Funct. Mater.*, 2020, **30**, 1910748.
- 269 F. Song, Y. Kong, C. Shao, Y. Cheng, J. Lu, Y. Tao, J. Du and H. Wang, *Acta Biomater.*, 2021, **136**, 170–183.
- 270 J. Xiang, Y. Wang, L. Yang, X. Zhang, Y. Hong and L. Shen, *Int. J. Biol. Macromol.*, 2022, **196**, 1–12.
- 271 A. M. Behrens, M. J. Sikorski, T. Li, Z. J. Wu, B. P. Griffith and P. Kofinas, *Acta Biomater.*, 2014, **10**, 701–708.
- 272 B. Tao, C. Lin, Z. Yuan, Y. He, M. Chen, K. Li, J. Hu, Y. Yang, Z. Xia and K. Cai, *Chem. Eng. J.*, 2021, **403**, 126182.
- 273 Y. Hao, W. Zhao, H. Zhang, W. Zheng and Q. Zhou, *Carbohydr. Polym.*, 2022, **287**, 119336.
- 274 Y. Hao, C. Yuan, J. Deng, W. Zheng, Y. Ji and Q. Zhou, *ACS Appl. Mater. Interfaces*, 2022, **14**, 16006–16017.

